Review

Stefan Mühlig*, Alastair Cunningham, José Dintinger, Toralf Scharf, Thomas Bürgi, Falk Lederer and Carsten Rockstuhl

Self-assembled plasmonic metamaterials

Abstract: Nowadays for the sake of convenience most plasmonic nanostructures are fabricated by top-down nanofabrication technologies. This offers great degrees of freedom to tailor the geometry with unprecedented precision. However, it often causes disadvantages as well. The structures available are usually planar and periodically arranged. Therefore, bulk plasmonic structures are difficult to fabricate and the periodic arrangement causes undesired effects, e.g., strong spatial dispersion is observed in metamaterials. These limitations can be mitigated by relying on bottom-up nanofabrication technologies. There, self-assembly methods and techniques from the field of colloidal nanochemistry are used to build complex functional unit cells in solution from an ensemble of simple building blocks, i.e., in most cases plasmonic nanoparticles. Achievable structures are characterized by a high degree of nominal order only on a shortrange scale. The precise spatial arrangement across larger dimensions is not possible in most cases; leading essentially to amorphous structures. Such self-assembled nanostructures require novel analytical means to describe their properties, innovative designs of functional elements that possess a desired near- and far-field response, and entail genuine nanofabrication and characterization techniques. Eventually, novel applications have to be perceived that are adapted to the specifics of the self-assembled nanostructures. This review shall document recent progress in this field of research. Emphasis is put on bottom-up amorphous metamaterials. We document the state-of-the-art but also critically assess the problems that have to be overcome.

Keywords: metamaterials; plasmonics; self-assembly; nanochemistry; bottom-up; amorphous structures; plasmonic nanoparticles.

Falk Lederer and Carsten Rockstuhl: Institute of Condensed Matter Theory and Solid State Optics, Abbe Center of Photonics, Friedrich-Schiller-Universität Jena, D-07734 Jena, Germany

Edited by Harald Giessen

1 Introduction

The fusion of the fields of colloidal nanochemistry and nanooptics has fostered the emergence of an entirely new scientific area that deals with self-assembled plasmonic nanostructures. In this field, chemical self-assembly techniques are applied to fabricate nanostructures required for applications in optics and photonics. The primary goal of these bottom-up techniques is the fabrication of unit cells tailored at the nanoscale to exhibit a desired optical response in the visible and near infrared (IR) regime. Plasmonic nanoparticles (NPs), such as nanospheres or nanorods, serve as the tiny building blocks that the unit cells are made from. The localized surface plasmon polariton resonances (LSPRs) of the NPs in the visible and near IR can be exploited to achieve an optical response that differs dramatically from that of a diluted metal. Moreover, to observe a response from the unit cell that does not just correspond to that of an electric dipole of an isolated NP, the coupling of two or more NPs in a unit cell has to be achieved. If strongly coupled, the emergence of new resonances will be observed and changing the geometrical parameters of the entire arrangement allows for the tuning of all properties such as resonance position, resonance strength and lifetime. Therefore, the ultimate problem that has to be solved is the sufficiently dense arrangement of the NPs in a desired geometry.

The pioneering work by Alivisatos et al. [1] and Brousseau et al. [2] demonstrated the possibility of arranging two strongly coupled nanospheres (sometimes termed a dimer) with nanometer precision using DNA and molecular linkers, respectively. These first demonstrations of the fabrication of a unit cell by self-assembly initiated an enormous effort to design more complex nanostructures by bottom-up techniques [3–6]. The entire stream

^{*}Corresponding author: Stefan Mühlig, Institute of Condensed Matter Theory and Solid State Optics, Abbe Center of Photonics, Friedrich-Schiller-Universität Jena, D-07734 Jena, Germany, e-mail: stefan.muehlig@uni-jena.de

Alastair Cunningham and Thomas Bürgi: Départment de Chimie Physique, Université de Genève, CH-1211 Genève, Switzerland José Dintinger and Toralf Scharf: Optics and Photonics Technology Laboratory, Ecole Polytechnique Fédérale de Lausanne (EPFL), CH-2000 Neuchatel, Switzerland

of research gained momentum upon appreciating that these unit cells made from a small number of plasmonic NPs are still much smaller than the wavelengths of interest. Consequently, if the spatial density of unit cells is sufficiently high, the propagating light will not sense every individual unit cell but rather an effective medium. The properties thereof are dominated by the scattering properties of the individual unit cells. The emerging materials are called metamaterials (MMs). Metamaterials in general, and particularly bottom-up metamaterials, promise to significantly widen our opportunities to control the propagation of electromagnetic fields in these materials. One key prerequisite in obtaining MMs that qualitatively deviate from natural materials is to achieve a scattering response from the unit cells that corresponds to that of a magnetic dipole; thus leading to artificial magnetism. It therefore constitutes a primary research goal to identify unit cells that possess such a scattering response.

In general, all bottom-up MMs can be divided into two distinct groups with respect to the spatial arrangement of the unit cells. Metamaterials of the first group exhibit a deterministic arrangement of a huge number of unit cells in space, i.e., their position is not amorphous. This group is termed the long-range order group. It has to be stressed that the unit cell arrangement is not restricted to a periodic or quasi-periodic one. As long as there exists any type of ordering, e.g., the unit cells are arranged along chains but these chains do not exhibit any specific symmetry to each other, the MM belongs to this group. Metamaterials of the second, the short-range order group, comprise all MMs which can be fabricated by bottom-up techniques where self-assembly is only controllable at the short-range scale being necessary to built-up the single unit cell. However, their spatial arrangement cannot be controlled anymore and the material is, hence, usually amorphous.

One important example for fabricating long-range order bottom-up MMs is the technique of block-copolymer self-assembly [7–12]. Different polymer blocks are covalently bound to each other which allow them to assemble into well-defined geometries. The MMs are achieved by doping the block-copolymer with plasmonic NPs. Another approach for long-range ordering is based on liquid crystals as a host medium for the NPs [13-18]. An advantage of the latter technique is the tunable anisotropy of the liquid crystal host that can be exploited to control the LSPR of the incorporated NPs. Fabrication techniques that allow solely short-range ordering can also be adapted to achieve long-range order bottom-up MMs. This can be done in combination with additional fabrication techniques. A prominent example is the use of DNA [19] to self-assemble plasmonic NPs which normally works at a short-range

scale. A combination of DNA self-assembly with evaporation [20] or substrate pattering [21] yields long-range order bottom-up MMs. The same effect can be achieved by polymer ligands (to assemble the single unit cell) in combination with an entropy-driven drying mediated process [22, 23]. Apart from these combined techniques, the evaporation of solutions containing the plasmonic NPs allows the assembling of ultra-large scale arrays of NPs [24]. Additional substrate pattering opens the route to more sophisticated geometries [25] such as stripes [26], cylinders [27] or rings [28] made of densely packed NPs. This technique of pre-structuring the substrate is commonly referred as template self-assembly [29]. In principle, most chemical self-assembly techniques that lead to short range order can be adapted to offer long-range order as well by using well-defined template substrates. This is not restricted to the technique of evaporating a solution including the NPs (where the capillary force drive the self-assembly of the NPs) although this technique is very common [30, 31]. Furthermore, long-range ordering can be induced by a properly chosen geometry of the single NPs. It has been demonstrated that polyhedral silver NPs assemble into the densest packing and exotic lattices by a sedimentation process [32, 33]. Even complicated symmetries, such as quasiperiodic crystals, have been demonstrated by chemical self-assembly techniques [34].

Regarding the group of short-range ordering, one promising example is the evaporation of a solution containing the NPs onto a substrate to assemble them into a desired geometry of the unit cell. Commonly the NPs are coated in preceding process steps by a polymer to define the interparticle distance with nanometer precision and to control the optical coupling [35]. Various geometries such as trimer [36], heptamer [31, 35] and quadrumer clusters [37] have been demonstrated. Another way to form a unit cell with NPs is to use DNA [38]. First principle demonstrations [1, 39] were extended towards more sophisticated geometries [40], such as again, trimer [41] and tetramer clusters [42], binary mixtures of NPs [43], dimers made of asymmetric NPs [44], heteropentamer NP clusters [45], and chains of NPs [46], to name just the most prominent examples. These unit cells usually appear as planar structures on a substrate. However, using DNA it becomes possible to fabricate three-dimensional unit cells, as demonstrated for Janus particles [47]. Three-dimensional unit cells can also be achieved by more sophisticated techniques such as, e.g., DNA-guided crystallization [48], using DNA scaffolds [49] or DNA origami [50-53]. Another short-range ordering technique is based on organic molecular linkers to assemble the NPs. Various structures such as dimers and trimers [2], pyramidal structures [54], or larger aggregates were demonstrated [55-57]. Apart from that, electrostatic forces can be exploited to assemble the NPs [58]. Various unit cells either [59-62] two- or three-dimensional [63-66] have been realized. An in-depth overview of this technique is given in chapter 4. The directional solidification of eutectics has been exploited to fabricate split-ring resonator-like structures [67] and polaritonic MMs for THz applications [68]. Recently, self-assembly on the short-range scale was also demonstrated by introducing defect states into liquid crystals [69].

Regarding both groups of bottom-up MMs (the longand the short-range order group) the following remarks hold. Almost all bottom-up MMs are made of nanoscale plasmonic NPs as the building block for the unit cells. This constitutes a major difference to conventional MMs which are commonly fabricated by top-down nanofabrication technologies such as e.g., focused electron- or ion-beam lithography. There, the unit cells normally consist of elongated metal wires or plates or more complex shaped blocks of bulk metal. Therefore, the design concepts, the theoretical description and the simulation techniques regarding bottom-up MMs cannot be adopted from top-down MMs. Naturally, fabrication is completely different and the only aspect that might be shared by top-down and bottom-up MM concerns the optical characterization. A short comparison between top-down and bottom-up MMs is given in

chapter 6. Last but not least it has to be mentioned that much work has been published dealing with self-assembly of plasmonic NPs where the optical response of the final structure was not considered at all. Of course the fabrication of samples with a desired or tailored optical response increases the level of complexity compared to a mere demonstration of the fabrication of the samples. Therefore, in chapters 1 and 4 the focus of this review is the possible geometries of unit cells that can be achieved by selfassembly techniques. As such, studies where the optical response was not considered and it is not clear if the selfassembled structures are really bottom-up MMs are also discussed. In all other chapters where self-assembled MMs are in the focus of interest only references are given where the optical response was also investigated.

The aim of this review is to provide a general overview on the issues introduced above and is structured as follows. The next chapter includes novel theoretical models and simulation techniques to describe the scattering response of bottom-up MMs. In chapter 3 representative examples of unit cell geometries are presented along with a discussion of their optical properties. The focus is on bottom-up MMs that offer a magnetic dipole resonance. Chapter 4 describes in detail chemical fabrication techniques to achieve bottom-up MMs while chapter 5 outlines most established optical characterization techniques.

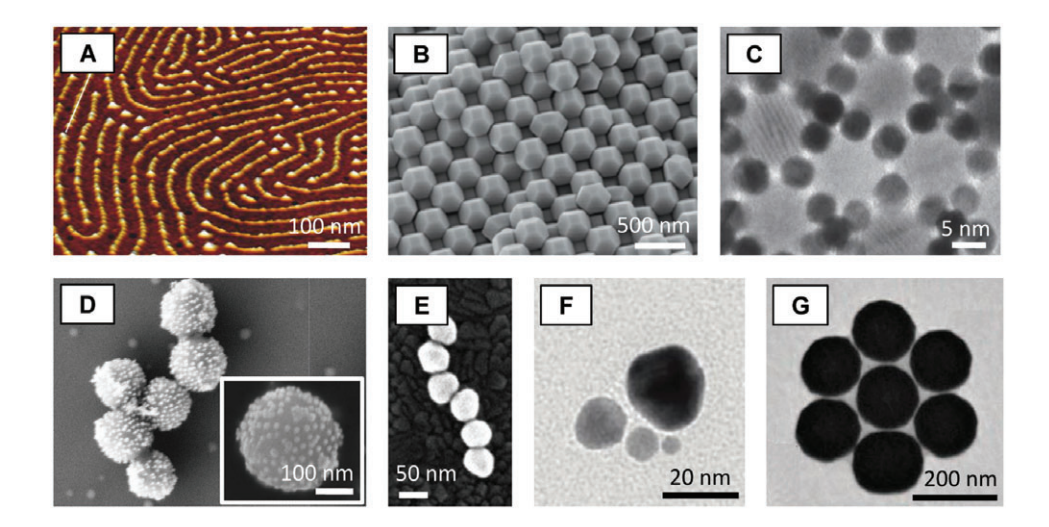


Figure 1 Self-assembled MMs exhibiting long-range (A)–(C) and short-range order (D)–(G). (A) Scanning force micrograph of spherical TiO, NPs self-assembled by block-copolymers. Reprinted with permission from Ref. [11], ©2011 by American Chemical Society (ACS). (B) Scanning electron micrograph (SEM) of self-assembled Ag truncated octahedral NPs by sedimentation. Reprinted with permission from Ref. [32], ©2011 by Macmillan Publishers Limited. (C) Transmission electron micrograph (TEM) of a self-assembled dodecagonal quasicrystal made of a binary mixture of Au und Fe₂O₂ NPs. Reprinted with permission from Ref. [34], ©2009 by Macmillan Publishers Limited. (D) SEM image of plasmonic core-shell clusters made of Au NPs self-assembled to dielectric core spheres by electrostatic forces. Reprinted with permission from Ref. [63], ©2011 by ACS. (E) SEM image of a self-assembled Au NP chain using DNA. Reprinted with permission from Ref. [46], ©2011 by ACS. (F) TEM image of Au NPs self-assembled into a chiral pyramidal structure by DNA. Reprinted with permission from Ref. [49], ©2011 by ACS. (G) TEM image of an Au heptamer cluster self-assembled by evaporation. Reprinted with permission from Ref. [35], ©2010 by American Association for the Advancement of Science (AAAS).

Chapter 6 gives a short overview of applications of bottomup MMs along with a description of problems that have to be solved in the near future. This chapter also describes future perspectives and routes how to further advance this important field of nanoscience.

2 Theoretical concepts and numerical means to quantify the optical properties

Most long-range ordered self-assembled MMs are made of unit cells that consist of a single plasmonic NP [see Figure 1(A)–(C) and Figure 2]. This causes an optical response of the MM that is mainly dominated by the excitation of the LSPR in the NPs. Therefore, the expected resonance features of such a material are limited. In contrast, the group of short-range order self-assembled MMs consist of complex unit cells that contain a huge number of plasmonic NPs [see Figure 1(D)–(G) and Figure 2]. This entails (due to strong coupling between NPs within the unit cell) a more complex response of the unit cells such as e.g., those of magnetic dipole [63] – or Fano type [35] resonances. That is why the optical response of the entire material can be tailored for a specific desired application.

The idea of MMs is based on having a structure at hand that is made from complex unit cells which sustain a tailored optical response. A primary issue in MM research is the desire to describe light propagation in such complex structures by simple constitutive relations, as known for conventional materials such as, e.g., dielectric media or metals. Potentially a quite general approach that is used for MMs are the so-called biisotropic, local constitutive relations. They relate the electric and the magnetic field to the dielectric displacement and the magnetic induction. In temporal and spatial frequency domain these constitutive relations can be written as

$$\mathbf{D}(\mathbf{k},\omega) = \varepsilon_0 \varepsilon(\omega) \mathbf{E}(\mathbf{k},\omega) + \frac{i}{c} \kappa(\omega) \mathbf{H}(\mathbf{k},\omega),$$

$$\mathbf{B}(\mathbf{k},\omega) = \mu_0 \mu(\omega) \mathbf{H}(\mathbf{k},\omega) - \frac{i}{c} \kappa(\omega) \mathbf{E}(\mathbf{k},\omega),$$
(1)

where the following material parameters are introduced: $\varepsilon(\omega)$ and $\mu(\omega)$ as the permittivity and permeability, respectively, and $\kappa(\omega)$ as the magneto-electric coupling. These constitutive relations can easily be extended towards the anisotropic case. Then all material parameters become tensors. The important approximation to mention here is the assumption that the material parameters do not depend on the spatial frequency k, which is usually assumed for MMs [70]. In this case Eq. (1) can be easily rewritten as local equations in real space, i.e., for all fields as a function of (\mathbf{r}, ω) . The dependency on \mathbf{k} is called spatial dispersion. Physically, this describes a dependency of the material parameters on the wavevector which can be the propagation direction of light through the MM or the angle of incidence. Such a dependency is undesired in any case. The material parameters should not depend on the propagation direction of the incident field. Alternatively, a product in Fourier space would correspond to a convolution in real space. Then, it is obvious that the material acts non-locally. This suggests that the electric displacement or the magnetic induction at a certain site depends also on the electric or magnetic field at adjacent sites. This is something which is not observed in ordinary optical materials such as conventional dielectrics or metals; and would actually create problems while formulating appropriate boundary conditions. There are two physical mechanisms in MMs that can cause this spatial dispersion.

The first one is related to a strict periodic arrangement of the unit cells of a MM. This is frequently encountered for top-down MMs that are normally planar, periodic structures. Thus, the periodic arrangement constitutes a grating, and the optical response should depend on the angle of incidence of the incoming light, which is indeed spatial dispersion. More generally, the origin of spatial dispersion is the resonant coupling of the near fields of adjacent unit cells due to their strict periodic arrangement. In this respect, short-range ordered self-assembled MMs possess an enormous advantage. Since the spatial arrangement of unit cells is amorphous, the optical response of these materials is not affected by spatial dispersion. Furthermore the amorphous arrangement causes an isotropic response. An incoming electromagnetic field always probes the same material independent of the propagation direction and its polarization. On the other hand this amorphous arrangement of unit cells implies a further complexity. The theoretical description of these materials is extremely challenging. In principle, the interactions of all unit cells that are illuminated by the incident electromagnetic field have to be considered. This is in most cases an unsolvable task. Furthermore, the amorphous arrangement increases parasitic scattering of the MMs [71]. In periodic top-down MMs the light can usually only scatter in well-defined diffraction orders (as dictated by the grating) which is not the case for an amorphous arrangement. Therefore, amorphous MMs suffer from an increase of radiative losses when compared to their periodic counterpart.

The second physical effect that can cause spatial dispersion is linked to higher order multipole moments of

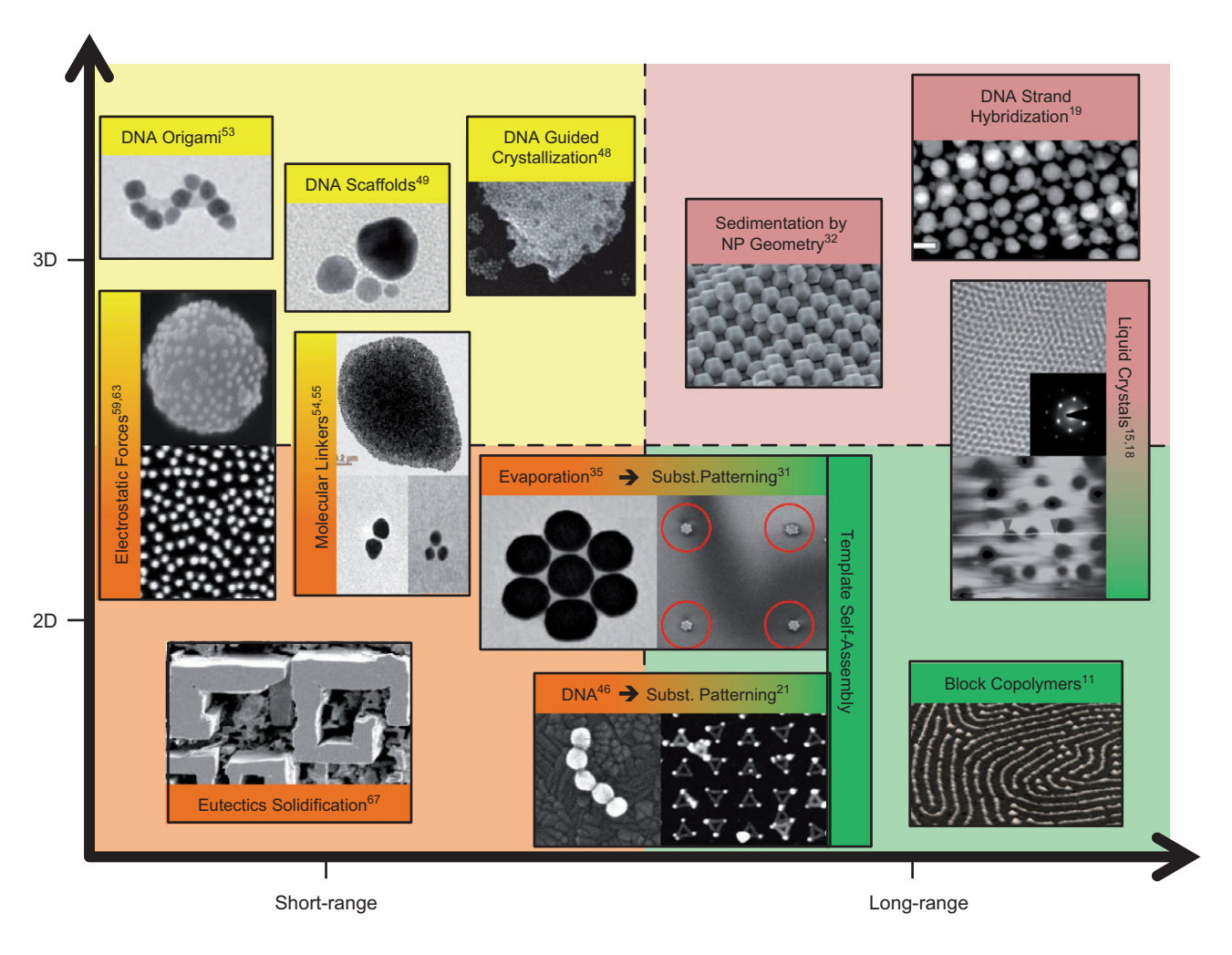


Figure 2 Schematic diagram of a selected set of self-assembly techniques. The images of the fabricated structures are arranged with respect to the spatial order of the unit cells on the x-axis and their dimension on the y-axis. On the bottom left self-assembly techniques are shown that result in short-range ordering and two-dimensional unit-cells, such as, e.g., directional solidification of eutectics (reprinted with permission from Ref. [67], ©2010 by Wiley-VCH), electrostatic forces (reprinted with permission from Ref. [59], ©2011 by ACS), molecular linkers (reprinted with permission from Ref. [54], ©2000 by ACS), evaporation of solutions including NPs (reprinted with permission from Ref. [35], ©2010 by AAAS), and DNA self-assembly (reprinted with permission from Ref. [46], ©2011 by ACS). On the top left techniques are shown that provide short-range ordering, but three-dimensional unit-cells. Electrostatic forces (reprinted with permission from Ref. [63], ©2011 by ACS) as well as molecular linkers (reprinted with permission from Ref. [55], ©2011 by OSA) can be adapted to offer both two- as well as three-dimensional unit cells. Therefore they appear in both quadrants. Furthermore, DNA based techniques such as DNA origami (reprinted with permission from Ref. [53], ©2012 by Macmillan Publishers Limited), DNA scaffolds (reprinted with permission from Ref. [49], ©2009 by ACS) or DNA guided crystallization (reprinted with permission from Ref. [48], ©2008 by Macmillan Publishers Limited) allow three-dimensional unit cells offering short range order. On bottom right techniques that allow for two-dimensional unit-cells that offer longrange order are shown. Evaporation (reprinted with permission from Ref. [31], ©2012 by ACS) and DNA (reprinted with permission from Ref. [21], © 2010 by Macmillan Publishers Limited), as they appear in the short-range two-dimensional quadrant, can be adapted to offer long-range order by additional substrate patterning. This special technique is known as template self-assembly. In addition self-assembly techniques such as block copolymers (reprinted with permission from Ref. [11], ©2011 by ACS) and liquid crystals (reprinted with permission from Ref. [15], ©2010 by AIP) yield two-dimensional unit cells with long-range order. The latter one also allows for fully three-dimensional unit cells and therefore it appears on the top left as well (reprinted with permission from Ref. [18], ©2009 by Wiley-VCH) in one line with DNA strand hybridization (reprinted with permission from Ref. [19], ©2011 by AAAS) and sedimentation of NPs (reprinted with permission from Ref. [32], ©2012 by Macmillan Publishers Limited) that also allow three-dimensional unit cells with long range order.

the unit cells that contribute to the scattered field in addition to the electric and magnetic dipole moments. It is out with the scope of this review article, but it should be mentioned here for clarification, that spatial dispersion can be linked to the first and higher order derivatives of the electromagnetic field components [72]. Without proving this statement we want to relate it to the multipole moments of the unit cell. If the electric interaction energy $W_{_{el}}$ between

an external electric field and a given charge distribution is expanded into a Taylor series one gets the following terms (ignoring electric monopoles)

$$W_{el} \approx -\mathbf{p} \cdot \mathbf{E}(\mathbf{r}, \omega) - \frac{1}{6} \sum_{i,j} Q_{ij} \frac{\partial E_j(\mathbf{r}, \omega)}{\partial x_i} + \dots$$
 (2)

The electric dipole moment **p** interacts with the electric field and the electric quadrupole moment Q_{ii} with the first derivative of the electric field. In terms of MMs the electric field is the incident field and the multipole moments belong to the carrier density of the unit cells. Therefore, the second term is responsible for spatial dispersion. It will show up if the carrier distribution of the unit cell exhibits a quadrupole moment and if the unit cell is so large (mesoscopic) that the derivative of the field cannot be neglected across the unit cell. In practice, this entails the requirement that unit cells have to be designed such that they can be sufficiently well described by electric and magnetic dipole moments only. This is necessary because usually the frequently desired magnetic properties require mesoscopic sizes of the unit cell.

To sum up, in the field of self-assembled MMs that exhibit short-range order, spatial dispersion can only stem from higher order multipole moments of the unit cells. Therefore, the basic design strategy is to develop unit cells which optical response can be described by electric and magnetic dipole radiation but that is still complex enough to deviate from that of a dilution of pure NPs.

In this chapter we will concentrate on the theoretical description of the scattering response of self-assembled unit cells of MMs. This is the first step towards a deep understanding of how light interacts with the entire selfassembled MM. As has been shown in recent papers, the optical response of amorphous MMs is mainly dominated by the scattering response of their unit cells [71, 73, 74]. Therefore, it is essential to provide an appropriate description of their optical response. Since most of the design strategies from the field of top-down MMs cannot be adopted, new design rules based on theoretical models have to be put in place. In the following, several distinct theoretical models are presented highlighting their advantages and disadvantages in the description of the scattering response of unit cells. The focus lies hereby on models that allow the quantification of the excited multipole moments. This is, as will be shown later on, the most important aspect of designing the unit cells for desired applications of MMs.

A widely used model to describe the interaction of an incident field with a MM unit cell is based on a quasistatic model. Capacitance and inductance are used to mimic the unit cell as an electric circuit [75, 76]. This so-called LC

model can provide a very intuitive understanding of the excited resonances in the unit cell. Since it is based on a quasistatic approximation of Maxwell's equations, several problems can arise [77], which can be alleviated, e.g., by more sophisticated models considering radiation damping [78]. Nevertheless, the applied capacitance and inductance of the analytical model are unknown quantities and have to be fitted to describe the experimental spectra sufficiently well. Furthermore, since the LC model is a quasistatic model usually only electric and magnetic dipoles are considered and no information is provided about higherorder multipole moments that are excited in the unit cell.

Another model to describe the optical response of the unit cell is based on coupled oscillators [79]. The plasmonic entities of the unit cell are replaced by one or more oscillating currents. A multipole expansion technique relates these currents to excited multipoles. Therefore, also higher-order multipole resonances can be identified. In analogy to the LC model experimental results are required to obtain the unknown parameters of the model such as, e.g., the coupling strength of the oscillators.

Apart from these two widely used analytical models one can use a fully numerical solution of Maxwell's equations to describe the optical response of the unit cell. This can be done in time domain by the finite-difference time-domain (FDTD) method or in frequency domain by the finite-element method (FEM). By solving the problem numerically, the entire scattered field of the unit cell is at hand and no further assumptions have to be made. However, it is by no way straightforward to achieve a deep physical understanding of the excited resonances in the unit cell by investigating just the field distributions. In some cases it is possible by interpreting the near-field components [80, 81] but in general no complete access of the excited eigenmodes is feasible.

The so-called T-matrix method [82-84] can reduce the complexity of the numerical solution to a level where one can physically interpret the involved resonances. Therefore, the scattered field of the unit cell, as well as the incident field, is projected onto a full set of eigenfunctions in spherical coordinates, the so-called vector spherical harmonics (VSHs). This projection yields the complex coefficients of this expansion. The T-matrix relates the known expansion coefficients of the incident field to that of the scattered field. On the one hand, the advantage of this method is that one can describe the interaction of the incident field with the unit cell on the basis of eigenfunctions (the VSHs) which allows for physical interpretations. On the other hand, the T-matrix method is still too complex in the case of MM unit cells. Usually, for MMs only one excitation direction and polarization state is of interest, whereas the T-matrix contains the information

for an arbitrary incident field. Furthermore, it is relatively challenging to calculate the entire T-matrix. Analytical solutions can only be obtained for simple shaped objects such as spheres [85] or ellipsoids [86]. For a more complex unit cell the T-matrix has to be computed numerically [87]. Last but not least it might be hard to interpret the optical response of the unit cell based on the VSHs since they require spherical coordinates which appears to be an unnatural choice for most of the MM unit cells.

The last theoretical model that is described here in detail is termed multipole analysis of meta-atoms [88]. It is based on the T-matrix method. It will be shown that arbitrary excited multipole moments in Cartesian coordinates of the unit cell can be extracted if the scattered field is known from numerical simulations. These multipole moments in Cartesian coordinates are usually the language of preference to discuss the optical properties and to eventually draw conclusions on the effective properties of the MM.

In a first step, equivalent to the T-matrix method, the scattered field \mathbf{E}_{sca} at a certain frequency ω is expanded into the VSHs which consist of two orthogonal sets of eigenfunctions labeled N and M that span the entire space

$$\mathbf{E}_{sca}(r,\theta,\varphi) = \sum_{n=1}^{\infty} \sum_{m=-n}^{n} k^{2} E_{nm} \left[a_{nm} \mathbf{N}_{nm}(r,\theta,\varphi) + b_{nm} \mathbf{M}_{nm}(r,\theta,\varphi) \right],$$
(3)

where k is the wavenumber in the homogeneous, isotropic surrounding, a_{nm} and b_{nm} are the unknown complex expansion coefficients (they are called scattering coefficients from now on) and E_{nm} is a scaling factor. The expressions for the VSHs **N** and **M** as well as for E_{nm} can be found in Ref. [88]. Analytical formulas for the expansion coefficients are only available for highly symmetric scatterers such as spheres or ellipsoids [89, 90]. For a sphere the well-known Mie coefficients relate the expansion coefficients for the known incident field [for an decomposition into VSHs analogous to Eq. (3)] to the scattering coefficients [91]. If the unit cell of the MM is more complex, the scattered field has to be simulated by a devoted numerical technique and projected onto the VSHs as

$$a_{nm} = \frac{\int_{0}^{2\pi} \int_{0}^{\pi} \mathbf{E}(r=a) \mathbf{N}_{nm}^{\star}(r=a) \sin\theta d\theta d\varphi}{\int_{0}^{2\pi} \int_{0}^{\pi} |\mathbf{N}_{nm}(r=a)|^{2} \sin\theta d\theta d\varphi},$$

$$b_{nm} = \int_{0}^{2\pi} \int_{0}^{\pi} \mathbf{E}(r=a) \mathbf{M}_{nm}^{*}(r=a) \sin\theta d\theta d\varphi$$

$$\int_{0}^{2\pi} \int_{0}^{\pi} |\mathbf{M}_{nm}(r=a)|^{2} \sin\theta d\theta d\varphi$$
(4)

The asterisk indicates the complex conjugation. The integrals in Eq. (4) are performed on a virtual sphere with radius a that encloses the MM unit cell. The origin of the sphere coincides usually with the points of highest symmetry.

It is worth mentioning that the expansion of the scattered field in Eq. (3) is equal, except some prefactors, to a multipole expansion in spherical coordinates where the scattering coefficients are the multipole moments. These spherical multipole moments are transformed into Cartesian ones since this appears to be the natural choice for most of the MM unit cells. Furthermore, having Cartesian multipole moments at hand facilitates in most cases the identification of the physical origin of the excited eigenmodes in the unit cell. After some straightforward but cumbersome calculations one obtains the transformation rules from the scattering coefficients from Eq. (4) to the Cartesian electric and magnetic dipole moments, p and m, respectively [88]

$$\mathbf{p} = \begin{pmatrix} p_x \\ p_y \\ p_z \end{pmatrix} = C_0 \begin{pmatrix} (a_{11} - a_{1-1}) \\ i(a_{11} + a_{1-1}) \\ -\sqrt{2}a_{10} \end{pmatrix},$$

$$\mathbf{m} = cC_0 \begin{pmatrix} (b_{11} - b_{1-1}) \\ i(b_{11} + b_{1-1}) \\ -\sqrt{2}b_{10} \end{pmatrix},$$
 (5)

with $C_0 = \frac{6\sqrt{\pi i}}{cZ_0 k}$ where c is the velocity of light and

 Z_0 the free space impedance. As can be seen in Eq. (5) only the lowest order scattering coefficients [n=1 in Eq. (3)]contribute to the Cartesian electric and magnetic dipole moments. The transformation rules for higher-order multipole moments such as the electric quadrupole moment can be found in Ref. [88]. The presented method, which we term multipole analysis of meta-atoms requires the knowledge of the scattered field (from analytical formulas or a numerical simulation) of the MM unit cell. Then it is possible to derive all excited Cartesian multipole moments. These multipole moments can be related to the entire scattering cross section of the unit cell as shown in Ref. [88]. Thus, it is possible to develop new design rules for self-assembled unit cells of MMs as shown in the next chapter and to assign effective parameters to amorphous MMs. This latter issue has been discussed recently [71, 74] and is not included in this review. However, a robust model is to use the dipole moments of the unit cells in Eq. (5) to calculate effective parameters of the entire MM. This can be done by using the Clausius-Mossotti model [92] or some effective medium theories [93] to relate

Table 1 Summary of various theoretical methods that describe the scattering response of a MM unit cell.

Method	Experimental data	Type of description
LC model	Required (L,C)	Analytical
Coupled oscillators	Required (coupling strength)	Analytical
FDTD/FEM	Not required	Numerical
T-matrix	Not required	Combined
Multi pole-analysis	Not required	Combined

the multipole moments of the unit cells to effective parameters of the entire MM.

It is worth underlining that the multipole analysis of meta-atoms does not require experimental data to fit some unknown parameters since it is based on a numerical solution of the scattered field. Furthermore, the complexity of the complete electromagnetic field is reduced to Cartesian multipole moments. They provide a deep physical understanding of the excited resonances in the unit cells. The eigenfunctions of the expansion can be arbitrarily chosen and the multipole decomposition can be also performed for the sources of the fields, as shown in Ref. [94].

To conclude this chapter, we note that several theoretical methods to describe the scattering response of a self-assembled unit cell exist nowadays (a brief summary is given in Table 1). The most suitable one seems to be a combination of a numerical solution of the scattered field and a multipole analysis as shown in Eqs. (3)–(5). The next chapter will outline the advantages of this technique and present some representative examples of self-assembled unit cells of MMs. The focus is placed on unit cells that exhibit a magnetic dipole moment in the visible.

3 Prototypical structures and their unique properties

This chapter demonstrates the advantages of the previously introduced multipole analysis of meta-atoms. A selected set of self-assembled unit cells of MMs is discussed. The focus lies on the design of self-assembled unit cells that allow the excitation of a strong magnetic dipole moment in the visible. It is shown that by using the multipole analysis of meta-atoms design rules can be developed and a deep physical understanding of the observed resonances is achieved.

As outlined in chapter 1, almost all self-assembled unit cells of MMs are made of strongly coupled plasmonic NPs that are nearly spherical and can be treated as perfect

spheres in simulations. This assumption is valid, since silver or gold NPs with diameters smaller than the wavelength can be easily fabricated with a nearly spherical shape (c.f. chapter 4). Furthermore, the focus here is on unit cells of MMs and therefore only far-field properties are of principal interest. A deviation of the spherical shape of the NPs in experiments would only slightly change the far-field optical response though it can have detrimental effects on the near-field. Concerning the simulations of the scattered field of a unit cell the assumption of a spherical shape suggests a great advantage since quasi-analytical solutions of Maxwell's equations are possible for systems of nonintersecting spheres. The applied formalism is based on an extension of Mie theory [89, 90] where one obtains the scattered field of a cluster of spheres in terms of the VSHs as shown in Eq. (3). Therefore, the overlap integral of Eq. (4) is not required to be performed and one can directly transform the scattering coefficients to the Cartesian multipole moments [c.f. Eq. (5)]. Nevertheless, it has to be stressed here that the multipole analysis of metaatoms is possible for arbitrary unit cells of MMs as shown in the literature [74, 94].

In the following the investigated unit cells are characterized by calculating their scattering cross section (Csca). Afterwards, the multipole analysis is performed in such a way that the excited Cartesian multipole moments are calculated according to their contribution to Csca. In other words, the sum of all investigated multipole moments yields the scattering cross section. This procedure assures that all excited Cartesian multipole moments are taken into account. Thus, one can easily identify the contribution of individual multipole moments to resonances of the unit cell. The dependency of Csca on the Cartesian multipole moments can be found in Ref. [88].

As mentioned previously we want to focus here on unit cells that allow the excitation of a strong magnetic dipole moment in the visible. The first example, shown in Figure 3(A), comprises a single silicon sphere with 200 nm radius. In the wavelength range of interest, i.e., in the near IR, the permittivity of silicon is almost constant, real-valued and large (ε≈12) [95]. The Cartesian multipole moments, shown in Figure 3(A), are exactly as expected for a high permittivity dielectric sphere. The first order resonance at 1500 nm can be related to an excited magnetic dipole moment [96, 97]. The second order resonance at about 1100 nm is identified as electric dipole resonance and the third-order resonance at 1000 nm as magnetic quadrupole resonance. In principle, the magnetic dipole resonance at 1500 nm suffices to construct a MM exhibiting a dispersive permeability just by arranging silicon spheres with a relatively high filling fraction. The

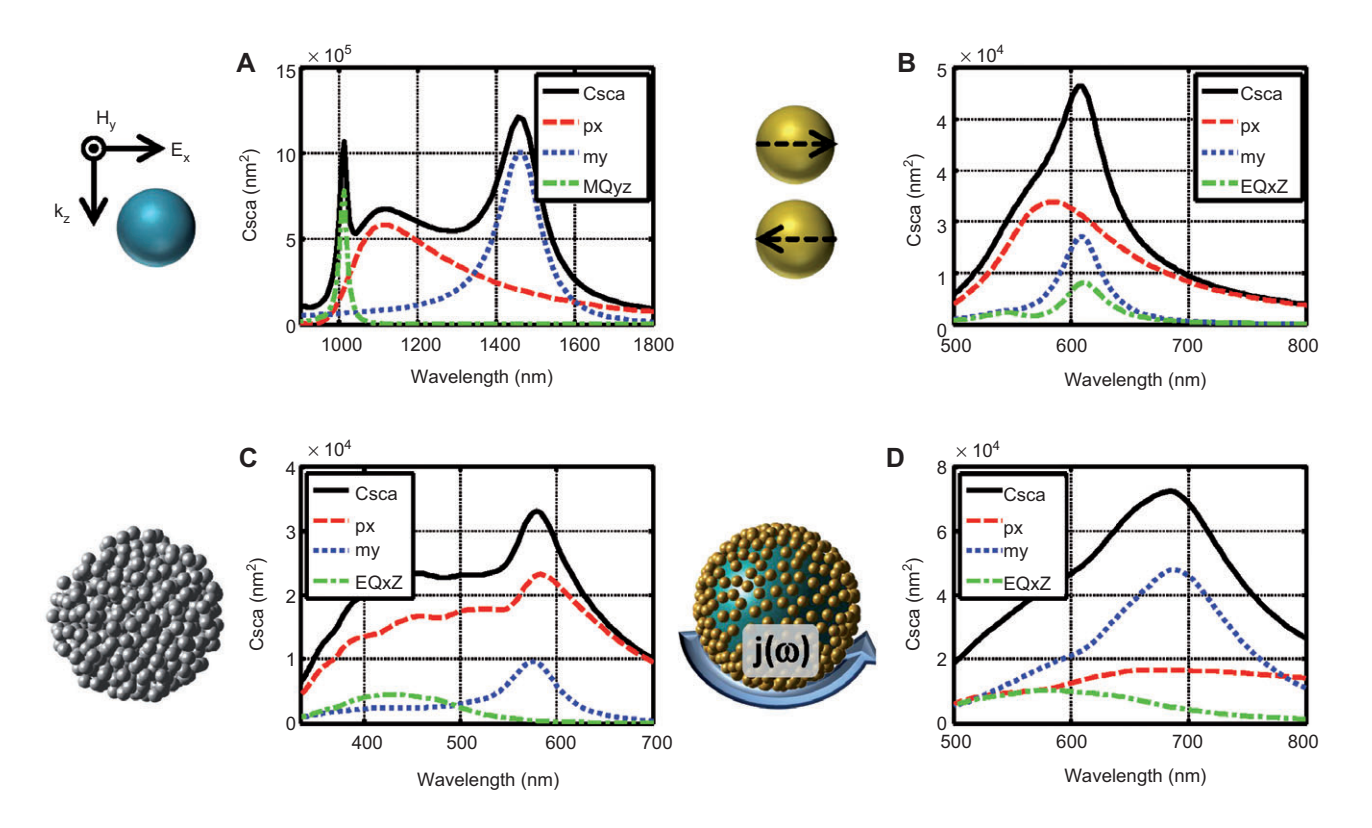


Figure 3 Multipole analysis of various self-assembled MM unit cells. The following Cartesian multipole moments are shown as a function of the wavelength: p – electric dipole, m – magnetic dipole, EQ – electric quadrupole, MQ – magnetic quadrupole as they contribute to the scattering cross section (Csca), (A) A single silicon sphere with 200 nm radius is illuminated by a plane wave as sketched. The illumination scenario is identical for all following unit cells. (B) Two strongly coupled gold NPs (40 nm radii and 5 nm separation) embedded in a dielectric with a permittivity of ε =2.25. (C) Self-assembled, amorphously arranged silver NPs (6 nm radii) form a cluster with spherical shape (75 nm radius) and are embedded in a dielectric (ε=2.6). (D) Self-assembled core-shell cluster made of a silica core sphere (130 nm radius) covered by a huge number of gold NPs (10 nm radii) forming a shell. The entire cluster is dissolved in water.

magnetic dipole moment in dielectric spheres is excited at frequencies where the wavelength inside the sphere is approximately equal to its diameter [98]. In other words, a single sphere that possesses a magnetic dipole resonance has to be made of a high permittivity material [98-104]. Using silicon carbide [105, 106] as the sphere material, the approach can only be implemented in the near IR or at even longer wavelengths. If the index is too low, such as for glass in the visible (ϵ =2.25), the excited magnetic dipole moment is too weak to induce a noticeable dispersion for the entire MM. Recent experiments have demonstrated the possibility of fabricating silicon spheres with diameters in the 50-100 nm range and therefore, shifting the magnetic dipole resonance [c.f. Figure 3(A)] to the visible [107, 108]. However, it is quite challenging to control the diameter of the silicon spheres in the experiments and therewith the accurate resonance position of the magnetic dipole resonance. Hence, in order to achieve a controllable and tunable strong magnetic dipole resonance in the visible more complex unit cells are required,

e.g., based on plasmonic NPs, as they are in the focus of this chapter.

The unit cell in Figure 3(B) consists of two strongly coupled gold NPs, sometimes termed a dimer, and also shows a magnetic dipole resonance in the visible. Each NP has a radius of 40 nm and, therefore, the scattering response of the single NP can be considered as purely electric dipolar. The resonance of this electric dipole is dictated by the excitation of the LSPR of the NPs and appears for gold in the visible. The coupling of the two NPs allows four possible eigenmodes [109, 110]. Two of these eigenmodes are symmetric, i.e., the electric dipoles in both NPs are oscillating in-phase to each other, and two of them are asymmetric, i.e., the electric dipoles are oscillating 180° out-of-phase. The illumination scenario in Figure 3(B) allows the excitation of one asymmetric eigenmode, illustrated by the dashed arrows. It is obvious that such an oscillation causes a magnetic dipole moment of the dimer [109, 110] that can be identified at around 600 nm in the shown spectra. The advantage is the appearance of this resonance in the visible since it is dictated by the LSPR resonance of the gold NPs. Furthermore, the spectral position of this resonance can be tailored by changing the distance between the NPs. However, one also observes a spectrally broad contribution of an electric dipole moment as well and the excitation of an electric quadrupole moment at the magnetic dipole resonance wavelength. The contribution of the electric dipole moment of the dimer to the scattering cross sections can be suppressed by tuning the dimensions of the NPs [111]. However, the non-negligible contribution of the electric quadrupole moment prevents the assignment of effective parameters to a MM made of these unit cells [72]. Furthermore, the entire structure is highly anisotropic, i.e., the magnetic dipole resonance only occurs for the presented illumination direction [88]. Of course an amorphous arrangement of the dimer unit cells in space will cause an isotropic response but the contribution of the magnetic dipole resonance to the optical response of the entire MM is decreased by a factor of 1/3. This is caused by the three independent orientations of the unit cell with respect to the propagation direction of the incident plane wave. Therefore, unit cells that provide an isotropic magnetic dipole resonance in the visible are desirable.

One potential solution to achieve this isotropic response is to arrange the NPs into clusters with a spherical outer shape, as shown in Figure 3(C) and (D). In the first example in Figure 3(C) the unit cell consists of amorphously arranged silver NPs (6 nm radii) that form a cluster with a spherical outer shape (75 nm radius) [55–57]. The magnetic dipole resonance can be identified at around 550 nm in the spectrum. The existence of this magnetic dipole moment can be understood as follows. A bulk material made of these tiny silver NPs sustains a Lorentzian resonance in the effective permittivity close to the LSPR wavelength of the isolated silver NP. At longer wavelengths the real part of the effective permittivity can reach high positive values depending on the filling fraction. Forming a spherical cluster from such material [as done in Figure 3(C)] resembles at longer wavelengths (compared to the LSPR wavelength of the silver NPs) the situation shown in Figure 3(A) where a homogeneous high-permittivity sphere was considered. Therefore, the first-order resonance of the spherical cluster is expected to be a magnetic dipole resonance [112]. This concept of magnetic resonances also exists for clusters with a cylindrical shape made of densely arranged NPs. These clusters have been successfully fabricated by template self-assembly [26]. The advantage of the unit cell in Figure 3(C) is the isotropic response due to the spherical cluster shape. Moreover, no significant contribution of the electric quadrupole moment occurs at the wavelengths of the magnetic dipole resonance. Furthermore, the spectral

position of the magnetic resonance can be tuned by the filling fraction of the silver NPs [55, 57]. Unfortunately, the magnetic dipole moment does not dominate the scattering cross section. A dominant contribution of the electric dipole moment is still present.

This problem is solved by the unit cell geometry in Figure 3(D), which is called a core-shell cluster. It consists of a silica core sphere (130 nm radius) that is decorated by a huge number of gold NPs (10 nm radii) forming a shell [63]. One way to explain the observed magnetic dipole resonance at about 700 nm in Figure 3(D) is the following. Each gold NP at the shell can be considered as a pure electric dipole. By illuminating this core-shell cluster by a plane wave all these electric dipoles at the shell can oscillate in-phase around the core sphere at a particular frequency. This causes an effective current in the shell as sketched by the blue arrow in Figure 3(D) that can be identified as a magnetic dipole moment [113, 114]. The advantage of the presented core-shell cluster unit cell is its isotropic response due to the spherical outer shape. Furthermore, in contrast to the unit cell in Figure 3(C), the magnetic dipole moment dominates the scattering cross section in the relevant wavelength range. Close to the magnetic dipole resonance wavelength the contribution of the electric dipole and quadrupole moment can be neglected. This dominating magnetic dipole moment stems from the reduced amount of metal in the unit cell compared to Figure 3(C) which reduces the absorption and sharpens the resonances.

To sum up, various unit cell geometries have been presented in this chapter that are made of spherical NPs and which allow the excitation of a magnetic dipole moment in the visible. By starting from a single NP, more complex geometries have been discussed.

Applying the multipole analysis of meta-atoms as presented in chapter 2, design rules have been developed to achieve a unit cell with a dominating magnetic dipole moment in the visible. The most promising unit cell geometries, as presented in Figure 3(C) and (D), have been fabricated by self-assembly techniques, and are presented in the next chapter. Here, we admit that there are other theoretical suggestions for magnetic dipole resonances in clusters of plasmonic NPs, based on trimer, quadrumer or tetramer clusters [115] or on two-dimensional rings of NPs [116, 117]. Magnetic resonances were demonstrated for selfassembled quadrumer and heptamer structures by DNA self-assembly [45]. However, these clusters (consisting only of a few plasmonic NPs) play a more important role for the generation of Fano resonances [35, 45] or large local field enhancements [118] for surface-enhanced Raman spectroscopy. However, this field of self-assembled plasmonic nanostructures is also rapidly growing and would require a separate review article. Therefore, this topic is disregarded here and the focus lies solely on self-assembled MMs.

4 Referential fabrication techniques

As described in chapters 1 and 2 the MMs fabricated using bottom-up methods possess several advantages over their top-down counterparts. As well as offering design benefits such as smaller feature sizes and more ready access to three-dimensional MMs, these techniques are, in general, cheaper and quicker. This is of prime importance for the eventual application of this technology. As such, over the last decades a significant amount of research effort has gone into the fabrication of plasmonic NPs using colloidal nanochemistry as the building blocks of the MM unit cells. This field, despite being relatively mature, is constantly being updated and NPs of a wide variety of shapes, sizes and composition can now be readily produced [38, 119]. This large catalogue of plasmonic materials, exhibiting LSPRs at optical frequencies [120], is becoming of increasing importance to the burgeoning field of optical MMs. When using such NPs to prepare structures with advantageous optical properties it is typically necessary to induce their organization, normally through the exploitation of particle-substrate and interparticle interactions, into specific architectures that have been proposed by theoretical models, as outlined in chapter 3. The development of novel and innovative methods combined with the manipulation of pre-existing ones allows this to be done. The field is too large to give a comprehensive review of all of the bottom-up methods used to both prepare plasmonic NPs and assemble them into structures that could be useful to the field of MMs. However, in chapter 1 a brief overview of some commonly used self-assembly techniques was given and they were categorized depending on the resulting arrangement of the unit cells in space. In this chapter an attempt will be made to introduce some of the primary techniques that have been used in this newly developing domain in more detail. Furthermore, the fabrication of two unit cell geometries that exhibit an isotropic magnetic dipole moment in the visible, as presented in chapter 3, is discussed here.

Due to their superior optical properties and their ease of handling, the majority of MMs use either silver or gold as plasmonic building blocks of the unit cells. Where bottom-up techniques are concerned, these NPs are generally fabricated by reducing a salt of the metal in question in solution. One of the most common methods used to produce metallic NPs with a nearly spherical shape is

known as the Turkevich method which was first developed in 1951 [121] and essentially involves the reduction of chloroauric acid by sodium citrate [122]. The citrate molecules play two roles in the synthesis; first reducing the metal ions to form the NPs and secondly forming a negatively charged capping layer at their surface which stabilizes them in solution and prevents them from aggregation. Here, the ratio of gold to citrate in solution defines the size of the particles and allows their diameters to be accurately controlled [122]. The Lee-Meisel method, in essence analogous to that described above, can be used to produce charged silver NPs [123]. Another referential technique used to prepare plasmonic NPs is the Brust-Schiffrin technique, a two-phase method which yields metallic NPs in an organic solvent [124]. In addition to NPs with spherical shape, plasmonic nanorods [125] can readily be synthesized using a seed-mediated method that involves the addition of small 'seed' particles to a growth solution containing a surfactant which stimulates preferential growth along certain crystal facets, resulting in elongated particles. Here, through the careful control of the growth conditions it is possible to tune the aspect ratio, and therefore the optical response, of the particles. Whilst being used less often in the assembly of bottom-up MMs, more exotic plasmonic NP geometries such as nanoshells and nanostars can readily be prepared using colloidal nanochemistry techniques [119].

Exploiting the coupling properties that these NPs possess and fabricating materials with tailored optical properties is one of the major motivations driving material scientists to find novel means to induce their self-assembly. The versatility of the NPs, largely resulting from the wide-ranging surface chemistry that can be used to cap them, means that a huge amount of techniques originating from disparate areas of chemistry can be used to this end. While a larger degree of flexibility can be gained by combining both bottom-up and top-down methods only strictly bottom-up techniques will be considered here. One of these techniques involves harnessing the inherent order that is present in liquid crystal systems to impart order on the NPs themselves, resulting in organized resonant inclusions in the host material [18]. This can be achieved by using one of two general approaches; either by simple mixing of the two species [126], or modifying the surface chemistry of the particles and functionalizing them with liquid crystalline ligands [15]. Whilst these self-assembly techniques work to a large extent they suffer from the relatively low solubilities of the NPs in the host and the maximum size of the particles that it is possible to incorporate, although it has been reported that particles of up to 7 nm in diameter have been included in such systems [15].

One of the most important examples of self-assembly exhibited in nature, that of the double helix structure of DNA, can also be used to organize plasmonic NPs. By engineering an interaction between the two, Alivisatos et al. pioneered the decoration of DNA templates with surface-modified gold NPs, producing dimers and trimers of well-defined separations [1]. Similarly, Chen et al. used a chemically modified peptide to reduce a gold salt, resulting in a left-handed arrangement of gold NPs along the peptide backbone [127] as is shown in Figure 4(A). The introduction of chirality to the organization of plasmonic NPs produces optically active materials and gives an additional means to tune the optical properties of such systems. More recently, DNA has also been used to engineer reproducible nanogaps between gold and silver NPs for the purpose of creating SERS active substrates [130]. Here, single molecule sensitivity of dye molecules inserted into the nanogaps was achieved showing that the applications of self-assembled plasmonic NP structures are not limited to the field of MMs and can be used

to fabricate nanooptical devices, such as nano-antennas, that mediate the interaction of light with molecular systems [131-139].

Synthetic polymers, as well as natural ones such as DNA, can also be used to induce the self-assembly of plasmonic NPs. A pseudo-ABA block copolymer system can be set up by selectively tethering polymer chains at the extremities of gold nanorods [129], as shown in Figure 4(C). By altering the solvent conditions, increasing or decreasing polarity, it is possible to induce either sideby-side or end-to-end organization of the rods which has a substantial effect on the coupling between them and therefore their resulting optical properties [140].

Several theoretical studies have shown (c.f. chapter 3) that spherical arrangements of plasmonic NPs are of significant interest to the MMs community due to the possibility of introducing magnetic resonances, a necessary building block of negative refractive index materials [112, 113]. By replacing the citrate capping shell that stabilizes gold NPs fabricated using the Turkevich method

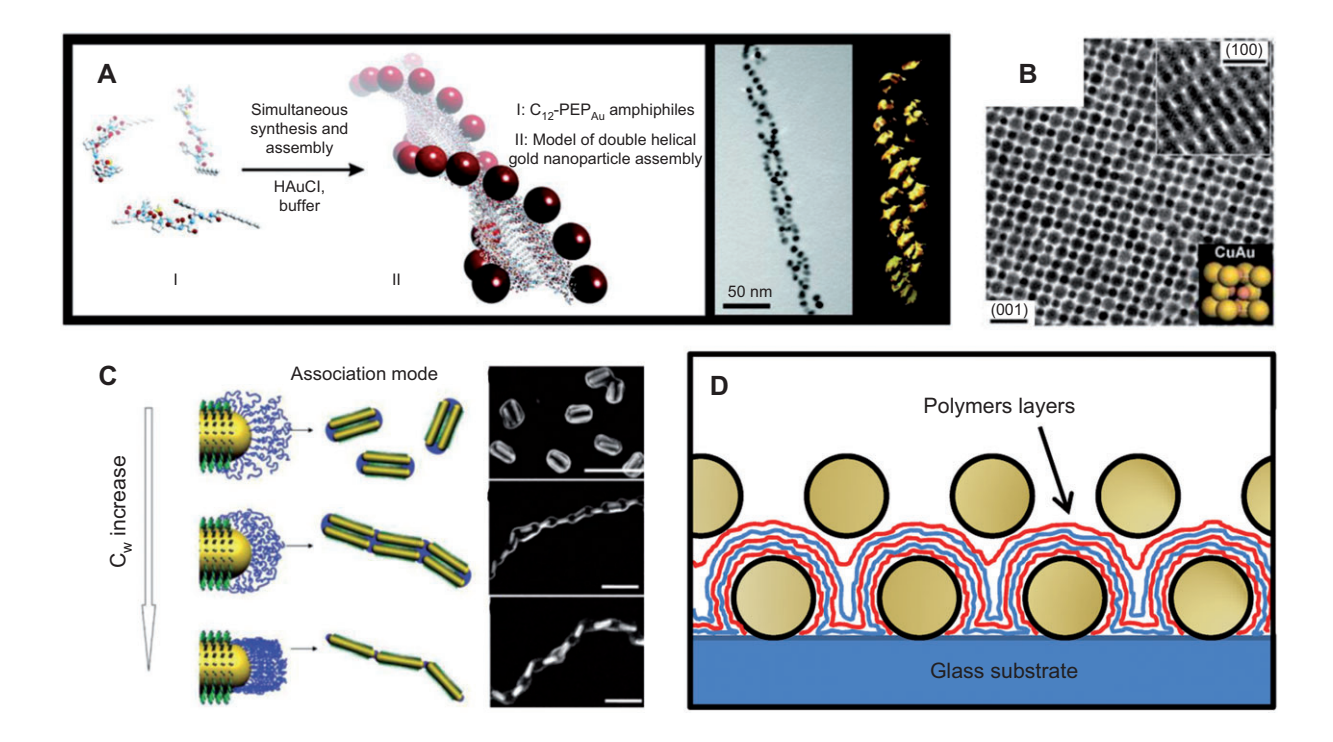


Figure 4 Various fabrication approaches for the organisation of metallic nanoparticles. (A) Gold nanoparticles that are both simultaneously synthesised and organised into double helical forms. Left - schematic principle of the method; right - electron microscopy images of the assembled structures. Adapted with permission from Ref. [127], ©2008 by ACS. (B) Au (5 nm) and PbSe (7.6 nm) binary nanoparticle superlattice prepared by colloidal crystallisation techniques. Unit cell shown in the inset. Reprinted by permission from Macmillan Publishers Ltd: Nature [128], ©2006. (C) A-B-A pseudo block copolymers prepared by selectively grafting polymers at the extremities of gold nanorods. Changing solvent conditions can alter the organisation of the particles. Adapted with permission from Ref. [129], ©2008 by ACS. (D) Graphical representation of two gold nanoparticle arrays separated by a number of polyelectrolyte layers. Separation between the arrays can be controlled with almost nanometre precision simply by altering the number of polymer layers. Reprinted with permission from Ref. [59], ©2011 by ACS.

with 11-mercaptoundecylether it is possible to provoke the self-organization of the particles into spherical clusters of around 1 µm in diameter [56]. These nanospheres, in turn, were also observed to assemble into larger structures, forming hierarchical arrangements of plasmonic NPs that closely resemble structures that have been proposed as possible negative permeability materials [112]. Other means, for example using oil-in-water emulsion technology, have also been used to produce unit cells of MMs by spherical arrangements of plasmonic NPs using bottomup methods [57]. Examples are given in Figure 5(A) and (B). Here, an oil-solution including silver NPs (6 nm radii) is mixed with water under constant stirring. This forms spherical oil droplets that are stabilized by a molecular linker. The resulting structures are spherical unit cells of amorphously arranged silver NPs. This unit cell has been proposed in chapter 3 [c.f. Figure 3(C)] to offer a magnetic dipole resonance at around 550 nm. This is verified by the measured extinction curves in Figure 5(E) where a red-shifted resonance (compared to the LSPR of the silver NPs) can be observed. Since this red-shifted resonance is unambiguously associated with the excitation of a magnetic dipole resonance, it is possible to create another possible building block for use in the fabrication of bulk MMs at optical frequencies by confining suitably functionalized particles to an oil phase that has been dispersed as small spherical globules in a non-miscible solvent such as water.

In general, most of the bottom-up self-assembly techniques result in amorphous structures that display no long-range order of the unit cells as discussed in chapter 1. This, however, is not always the case and interparticle forces arising from entropic, steric, dipolar and van der Waals contributions can be used to create binary

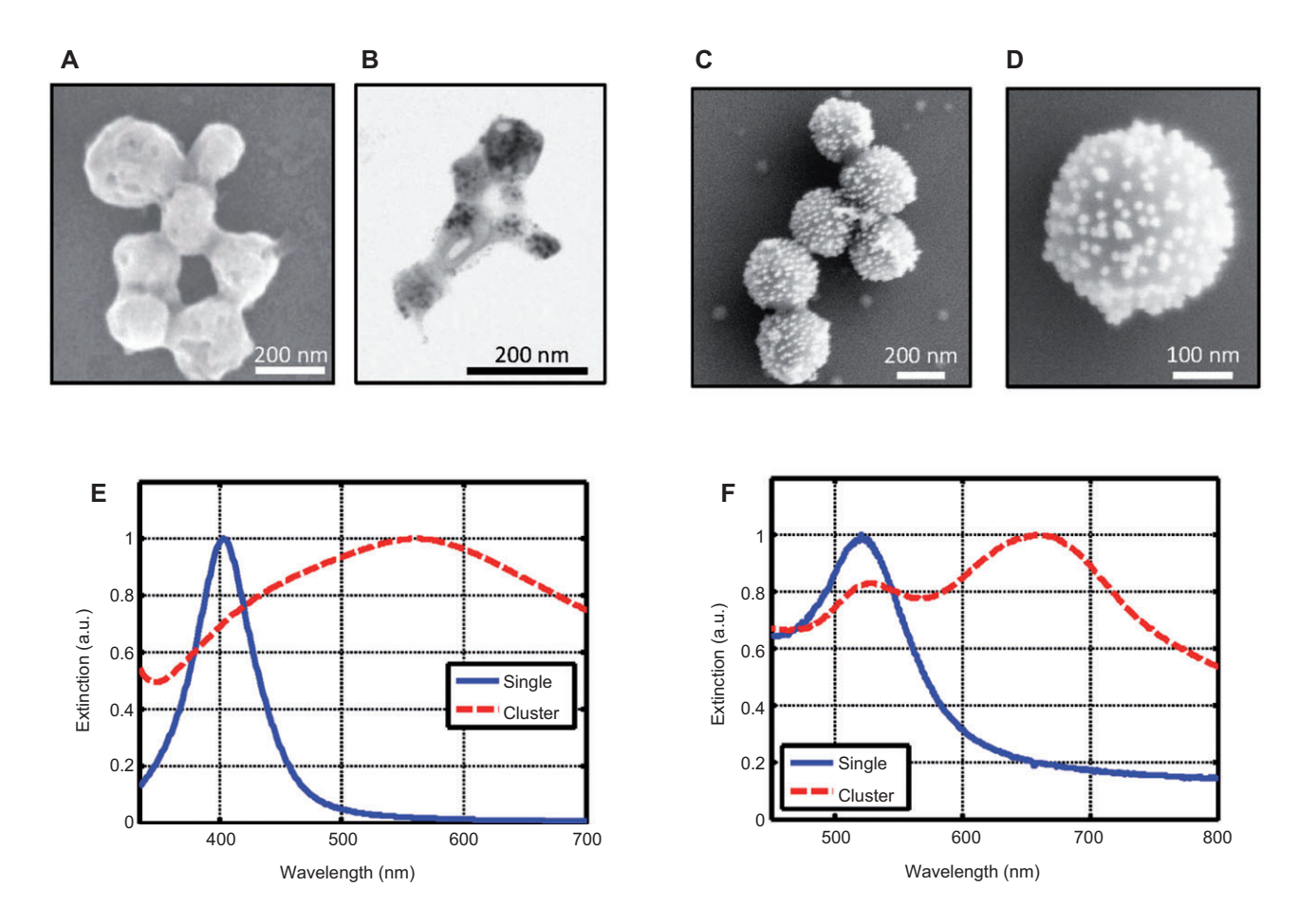


Figure 5 Fabricated self-assembled MM unit cells. In (A), (B) the MM unit cells are fabricated by a self-assembly technique based on oil-inwater emulsion. The SEM image in (A) shows the encapsulate of the spherical silver NP clusters whereas the TEM image in (B) reveals the formation of silver NP clusters with a spherical outer shape. In (C) and (D) SEM images of self-assembled core-shell clusters are shown. The core sphere consists of glass and a huge number of gold NPs are attached to the core by electrostatic forces forming the shell. In (E) and (F) the corresponding measured extinction spectra of the used plasmonic NPs (blue solid curves) as well as of the self-assembled MM (red-dashed curves) are shown for the spherical silver NP cluster and the core-shell cluster, respectively.

NP superlattices [128]. Made by colloidal crystallization methods and with precise control over the size, shape and composition of the NP inclusions achievable, optical, magnetic and electronic properties of the lattices can be engineered.

Another method which has shown impressive control over a wide range of material parameters is the combination of plasmonic NP deposition techniques with the layer-by-layer assembly of polyelectrolytes [141]. While the studies of layered adsorption of molecular species have existed for several decades, perhaps most notably using Langmuir-Blodgett or chemisorption techniques [142], several advantages exist when using charged polymers to build up thin films constructed from well-defined numbers of distinct layers. No special equipment is required and the method is quick, cheap, and applicable to a host of different situations. It essentially involves the deposition, on a charged substrate, of a polymer of opposite charge using nothing more than electrostatic interactions. After a washing step another polymer layer, again of opposite charge, can be deposited. The adsorption and washing process can be carried out in less than a minute, can be automated using a simple dip-coater and can be repeated in a cyclic manner as many times as is required for the purpose at hand. Materials such as silicon, glass and polydimethylsiloxane, selected for their electronic, optical and mechanical properties respectively, can be functionalized in a facile manner in order to induce the electrostatic interactions that are required for the use of this method [143]. Gold NPs prepared by the Turkevich method, as previously mentioned, display a negative surface charge and as such prove to be ideal candidates for inclusion in layered assemblies of charged polymer species [59, 144]. The flexibility offered by this technique is almost boundless. The size, composition and, to a certain extent, shape of the particles can be controlled as well as their lateral spacing, as sketched in Figure 4(D). Many distinct arrays of gold NPs as desired can be integrated into a large scale (cm2) dielectric host matrix with out-of-plane separations ranging from the nanometer scale upwards. This allows structures to be built into the third dimension and materials with true bulk properties to be prepared [59]. The wide variety of charged polymers, or indeed block copolymers, that are available with properties ranging from fluorescence to being redox active means that the origin of the functionality of such materials is not limited to the plasmonic NP inclusions [145]. This versatility allows precise designs with specific properties to be targeted. Using these techniques, and considering one of the more simple configurations (two arrays of well separated gold NPs separated by polymer layers), it can be

seen to what extent the optical properties can be tuned. By reducing the numbers of polymer layers separating them, the NP arrays approach one another. As the particles within a single array are sufficiently well separated the only particle-particle interaction will occur between the two distinct arrays. The strength of this interaction, strongly related to the interparticle distance [146], will increase exponentially as the arrays cross the coupling threshold and continue to approach one another. This results in ever increasing red-shifts of the plasmonic resonance that the particles exhibit [59]. When the particles approach to within extremely small distances, separated by a single polymer layer, it is even possible to access a splitting of the eigenmodes with a resultant dipole moment predicted by plasmon hybridisation theory [147]. The investigation of asymmetric layers of plasmonic NPs has demonstrated the possible excitation of so-called dark eigenmodes [62] under plane-wave incidence, which is only possible if the distance between the NPs is in the nanometer range, meaning the coupling between them is particularly strong.

An additional advantage afforded through the use of self-assembly fabrication techniques based upon electrostatic forces is that the structures are not limited to planar geometries. The techniques described above can be applied to substrates of any form. This is extremely valuable in terms of presenting flexible fabrication methods that can be employed in a variety of differing situations. This is particularly pertinent when the importance of spherical arrangements of plasmonic NPs to the field of MMs, as has been outlined previously, is taken into consideration. To this end, core-shell clusters can be fabricated using analogous methods to those described above, simply replacing the large scale planar substrates with microscale spherical ones [63], such as glass spheres. Of course in order to induce the electrostatic attraction between the core spheres and the negatively charged plasmonic NPs it is first necessary to functionalize the cores. This can be readily achieved, depending on the substrate material, using well established chemical reactions [143]. The example of a fabricated core-shell cluster from the SEM images in Figure 5(C) and (D) demonstrates the possibility of using this technique to decorate silica spheres (130 nm radius) with well separated monodisperse gold NPs [63] (10 nm radii). As before, it is possible to tune the size of both components as well as the density and composition of the NPs at the substrate surface, thus giving a high degree of control over the optical properties. The change in optical properties, between a solution of isolated gold NPs and a solution of the core-shell clusters, can be seen in the extinction

curves in Figure 5(F). The red-shifted resonance of the core-shell cluster was identified in chapter 3 by the excitation of a strong magnetic dipole moment [c.f. Figure 3(D)]. Thus, the presented MMs in Figure 5, whose unit cells are fabricated by self-assembly techniques, both exhibit an optical response to the magnetic field since magnetic dipole moments are excited in the unit cells. Therefore, they are first principle demonstrations of selfassembled MMs that exhibit a dispersive permeability, i.e., artificial magnetism.

A small snapshot, by no means comprehensive, of some of the principal bottom-up routes towards NP organization has been given in this chapter. This field is already considerably developed. However, the continual introduction of new techniques and their combination with existing ones means that this is an extremely fast moving area of research that is continually making notable advances. This indicates that only the surface has been scratched in terms of what can be achieved using self-assembly techniques and highlights both the power and versatility of the methods employed.

5 Optical characterization techniques

When measuring the optical response of composite materials several aspects need to be addressed. Although some of them do apply for all nanooptical materials, we concentrate here on materials made from an amorphous arrangement of complicated unit cells that are made from a larger number of plasmonic inclusions. In these materials, two characteristic lengths are important – the size of the basic element carrying a plasmonic resonance and the typical size of the inclusion in the composite. Throughout this review the resonances are caused by plasmonic NPs with a size range of 10-50 nm. From such NPs MM unit cells are formed that usually have a size smaller than or in the order of 300 nm. Although both sizes are smaller than the wavelength of light at optical frequencies, caution is necessary to correctly measure the characteristics of the material in the amorphous arrangement. However, since the optical properties of the composite are dominated by the scattering properties of the unit cell itself, the optical properties of the individual unit cell are of primary initial interest. The materials can be, therefore, characterized by two different approaches. On the one hand, measurement techniques can be used to probe the optical response of the entire material. On the other hand, techniques with high spatial resolution can be used to explore the characteristics of the isolated unit cell. Whereas the ensemble can usually only be characterized in the farfield, and the necessary techniques are summarized as whole-field techniques, in the latter strategy that probes the properties of individual unit cells, information can be acquired in the far-field but also in the near-field [148].

Due to this distinction this chapter is divided into two sections. Section 5.1 presents whole-field techniques that include measurements of transmission, reflection and absorption as well as ellipsometry. Section 5.2 presents techniques that probe single unit cells by scattering techniques, far field investigations, and optical near field measurement. It should also be stressed that not all of these characterization techniques were developed for self-assembled MMs. They can also be used and were, to a large extent, actually developed for deterministic structures.

5.1 Whole-field techniques

One can identify a number of standard techniques that are used for measuring material characteristics of large assemblies of unit cells in amorphous MMs: spectroscopy, interferometry and ellipsometry. The techniques become more powerful when combined and coupled with angular measurements. The most complete picture would be obtained in an instrument that gives access to amplitude and phase at all angles. Practically, this is not feasible and a number of special techniques have been introduced to make proper use of the results obtainable with only limited parameter variations. In classical whole-field techniques materials are characterized by beams that are much larger than an eventual unit cell or structure size of the investigated material. Beams are only weakly focused and are often considered as collimated with typical beam diameters in the mm range. Linked to the spatial collimation is an angular spectrum that has to be considered if the collimation is spatially too narrow. A measurement with such beams provides very high signal to noise ratio based on the fact that the systems generally have high throughput, i.e., the dark noise of the detector is compared with a large maximum signal.

The most common measurements taken to characterize materials are the measurement of transmission and reflection [149]. In principle, there are two different observation modes: specular/diffuse with direct observation and dark field observation when only scattered light is observed. A light beam is directed on a sample and the direct transmitted or reflected intensity (specular component or zero order) is analyzed. If the sample does not show any light diffusion the measurement provides reliable data on transmission, reflection and absorption. If diffusion is not explicitly considered (because it is neglected) one often speaks about extinction measurements. The extinction measurement is the standard characterization technique for self-assembled MMs in solutions. Using a model that describes the scattering properties of the unit cells it is possible to retrieve material characteristics of the NPs and meta-surfaces. Examples are given by Okamoto [150] and many others. If carefully done, a retrieval of effective material parameters is possible [151, 152]. This direct retrieval also requires, however, phase information which can be obtained only with devoted interferometers [153]. An example for a spectroscopic characterization can be seen in Figure 6. There, an SEM image from NPs on a subsrate is shown together with a measured extinction spectrum in solution and on a substrate. It can be seen and care has to be devoted to the fact that the presence of the substrate constitutes a modified dielectric environment for the NPs when compared to the solution. This changes the optical properties. In addition, agglomerations are observed on the substrate which also changes the plasmonic property due to coupling. A transmission measurement usually only provides basic information and does not allow the reconstruction of the internal structure of more complicated unit cells. Essentially, it only allows the probing of the spectral position of resonances and their line widths, i.e., lifetimes. However, if supported by simulations, more insight can be obtained, e.g., by a multipolar decomposition of the scattering response. If the filling

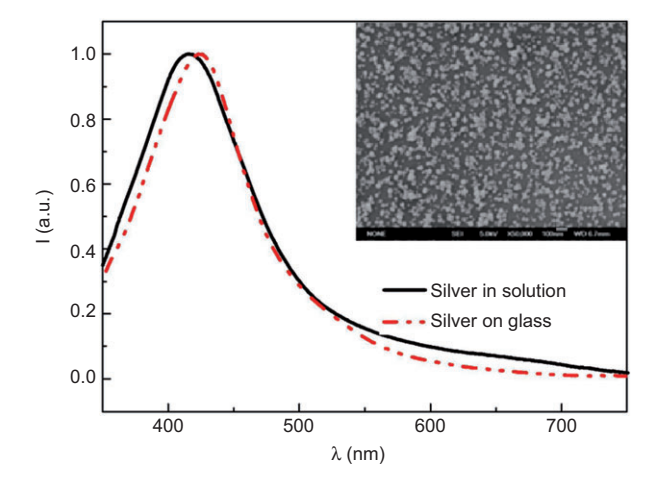
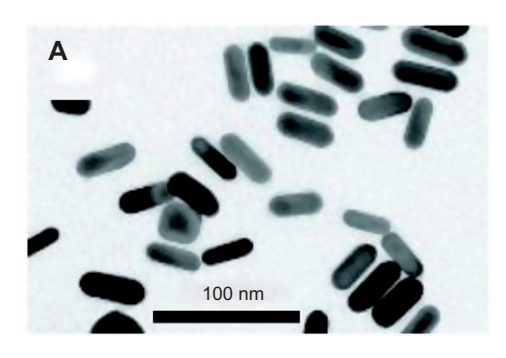


Figure 6 Extinction spectra of silver NPs in solution and on a glass substrate. The inset shows an SEM image of the silver NPs on the substrate. One clearly observes the formation of larger aggregates of NPs (which do not appear in solution) that modifies the extinction curve. Reprinted with permission from Ref. [154], ©2011 by Optical Society of America.

fraction of unit cells is not too high, the resonances of selfassembled MMs can be linked to the scattering properties of the single unit cells [71, 73, 74].

If the entire MM or the basic unit cell is anisotropic, polarization dependent spectroscopic investigations are a useful extension. To simplify the interpretations, these experiments are mainly performed at normal incidence to probe the extinction for different polarization directions. To this end, polarizers have to be introduced in the illumination and/or analyzing path of the spectrometer. Linear and circular extinction and dichroism measurements are the most common. A more advanced technique based on polarized light analysis is ellipsometry that is discussed next. The measurement of anisotropy is of particular importance for structures with inherent shape anisotropy of the basic plasmonic building block as it appears in nanorods for instance or in systems that form assemblies with reduced symmetry such as self-organized materials, i.e., liquid crystals. To observe particular effects for different polarization directions of light with conventional spectroscopy of large beams, the sample must show a macroscopic anisotropy. This suggests that some order needs to be found in areas as large as the beam size, as it appears in some self-assembled MMs with long-range order [c.f. Figure 1(A)]. In Figure 7 an example measurement is shown where a cigar-like shaped nanorod with an aspect ratio of $\eta \approx 2$ is investigated. Two peaks are distinguished that can be attributed to a LSPR along, and perpendicular to, the geometrical extension of the rod. If measured without a polarizer these two peaks can overlap (if the aspect ratio of the nanorods is not high enough) and might be no longer distinguishable. This is identical to the situation where a polarizer is used but an ensemble of arbitrary oriented nanorods is measured [156]. Therefore, as discussed in chapter 3, it is of great advantage to fabricate unit cells that offer an isotropic response. Then, all resonances of the unit cell can be obtained from ensemble measurements of the entire MM even if no fixed orientation between the unit cells exists.

A technique that makes explicit use of a polarization dependent response of the samples at oblique incidence is ellipsometry. It is a standard means to quantify the optical properties of self-assembled MMs prepared as thin films. The method is based on the measurement of the change of the polarization state at the surface of a sample at oblique incidence. Usually, different angles are used to enhance the quality of the analysis and it can be applied over the whole spectrum as spectroscopic ellipsometry. The evaluation of effective material parameters is based on sophisticated layer models. It is rather straight forward to apply for dielectric materials but needs to be carefully adjusted for



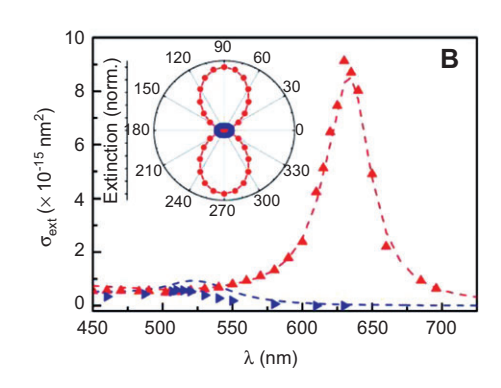


Figure 7 (A) TEM image of gold nanorods on substrate. (B) Single nanorod extinction measurements: computed (dashed lines) and measured (triangles) absolute values of the extinction cross section of a single nanorod for two linear polarizations parallel (red) or perpendicular (blue) to the main rod axis. The inset shows a polar plot of the computed extinction polarization dependence close to the longitudinal and transverse LSPRs at 640 and 525 nm, respectively. Reprinted with permission from Ref. [155], ©2008 by ACS.

materials with resonant entities. A recent review that summarizes findings when applied to plasmonic composite materials and especially MMs is documented in Ref. [157].

A more complete picture of the optical behavior of composite materials is obtained when interferometric techniques are used. They allow the measurement of optical quantities such as the amplitude and phase of reflected and transmitted light through a sample, respectively. The technique is challenging to implement since the phase measurement requires an absolute phase measurement, i.e., the phase has to be measured with respect to a referential phase. Only very few implementations are documented [153, 158].

Examples of two setups are shown in Figure 8. A classical interferometer of the Michelson type can be used to measure the effect of materials on the propagating phase [158]. Pulsed light is used and the measurement allows the determination of propagation properties such as phase and group velocities. Due to ambiguity of the measurement for large phase shifts only thin samples can be characterized. The measurement of reflection and transmission in amplitude and phase is possible with the setup shown in Figure 8(B). A fibered supercontinuum white light source is used to get highest quality of light and the spectrum is analyzed with an optical signal analyzer (OSA). The polarization interferometer of Jamin–Lebedeff type used in this experiment provides two beams with spatial separation where one is used as a reference [153].

With all these techniques it is possible to measure the far-field properties of an ensemble of unit cells. To

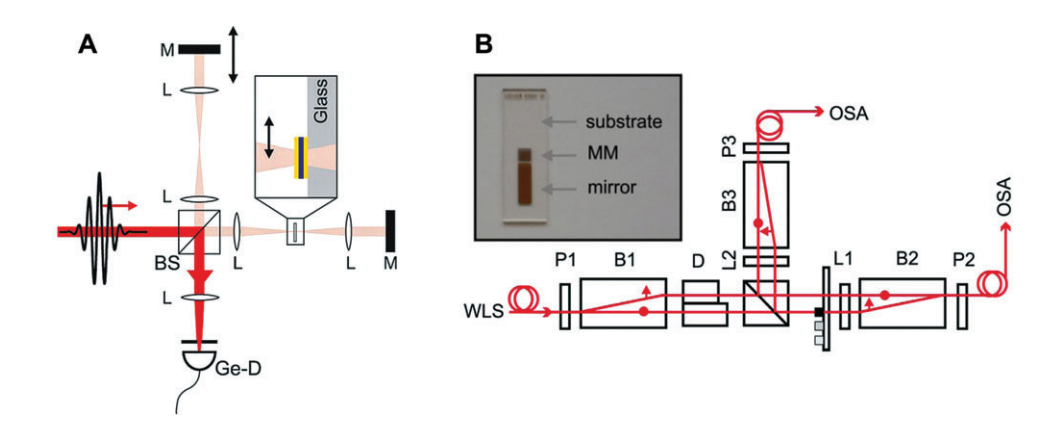


Figure 8 (A) Scheme of the experimental setup to measure the phase of transmission and reflection. A Michelson type of interferometer is used to detect propagation features of light pulses through thin films of MMs. M, mirror; L, lens; BS, beam splitter; Ge-D, germanium photodetector. The MM is on a substrate surface and can be moved in or out of the optical path. Reprinted with permission from Ref. [158], © 2006 by American Association for the Advancement of Science. (B) Interferometric setup to probe simultaneously transmission and reflection of samples. A polarization interferometer is used that allows to have a reference beam close to the sample. P1, P2, P3, polarizers; B1, B2, B3, beam displacers; L1, L2, half-wave plates; D, delay element. The insert shows the configuration of the experimental chip. Reprinted with permission from Ref. [153], ©2010 by Optical Society of America.

probe for the properties of the individual unit cells and to compare them to simulations as discussed in chapters 2 and 3, devoted techniques have to be put in place. They are discussed in the following.

5.2 Single unit cell characterization

A MM that aims to have a tailored optical response in the visible needs to be composed out of unit cells that are much smaller that the wavelength of light. In the special case of self-assembled MMs the amorphous arrangement of these unit cells implies the advantage that the optical response of the MM is mainly dominated by resonances of the unit cell itself and not by their arrangement. Therefore, the optical characterization of single unit cells plays a pivotal role to prove by experimental means that the optical response of the MM is dominated by the unit cell and, furthermore, to reveal and visualize the excited resonances in the unit cell. This leads to particular challenges in the characterization concerning the measurement area and the signal level, which both become very small. It is therefore useful to collect as much information as possible by accessing not only a single direction but looking at the scattered fields [159]. As scattering techniques we define here measurement principles that give access to angular distribution of light after interaction with the unit cell. The unit cell can be illuminated either directly or by using focusing lenses such as microscope objectives. One distinguishes direct illumination techniques and dark field illumination. Angular light distributions have typical signatures that depend on geometrical and material characteristics of the structure.

The evaluation of angular light diffusion characteristics can be done with a microscope by observing the back focal plane of the objective. The classical setup consists of the introduction of a Bertrand lens in the observation path known from the classical optical crystallography technique conoscopy [160]. This technique is used in polarization microscopy to identify the crystallographic axes of minerals and the orientation of optical axes in ordered systems like liquid crystals and polymers [161]. It is mainly used in transmission and at full numerical aperture illumination. Signal to background enhancement is given by the use of polarizers that are usually crossed. The interest of this method for material characterization is mainly structural investigations of assemblies of unit cells. A large variety of illumination techniques can be applied that lead to very different results and need careful analysis. That is the reason why in most of the experiments a well-defined

illumination (direction and wavelength) is used. Care has to be devoted to the matching of illumination and observation numerical aperture and the careful calibration of the system. An additional aspect is the signal to noise or background ratio of the measurement. Often, the scattered signal is weak and the direct illumination remains much stronger than the signal. It is therefore recommended to use contrast enhancement techniques like dark field illumination or cross polarization detection. If optically active substances are used, fluorescence can be explored by exciting and observing at different wavelengths to decrease the background signal.

A very exciting application of such techniques is the evaluation of a scattering cross section of a single split ring resonator (SRR) [162]. The SRR is brought into the focus of a microscope objective and illuminated with a Gaussian beam. The cross section of the investigated SRR would be too small to detect a signal. This problem is solved by time-periodic modulation of the SRR through the focus of the Gauss beam and a Lock-In amplifier setup. The two dimensional intensity distribution of the scattered field is evaluated by observing the back-focal plane of the objective. In the particular example two microscope objectives are applied, one for illuminating and a second one for observation.

As an example we show here the study of scattering properties of single metallic entities done with a total internal reflection excitation that deliver a high signal to background ratio. The total internal reflection technique for illumination additionally gives access to all types of resonances, i.e., the radiative or non-radiative ones [163]. In Figure 9 measurements were conducted with a numerical aperture of NA=0.95 which results in a certain range of the projected wave vector k_x and k_y depicted as the inner circle in Figure 9(B) and (C). The single nanobars are excited at 725 nm and with 200 µW. One should note that the false color scale for the two images differs by a factor of 10 [0–5 in (B) and 0–50 in (C)]. Single unit cells can be characterized but the method also allows the investigation of assemblies of functional units. Recently, the technique led to the the revealing of the magnetic nature of light emission by observing the angular distribution of the emitted light and by the evaluation of the angular momentum [164].

The desire to look into the local properties of the fields close to individual unit cells led to the application of optical near-field techniques based on scanning nearfield optical microscopes (SNOMs) [165]. This technique is established to study plasmonic materials in general and first experiments date back to 1989 [166–168]. In comparison to techniques presented so far, SNOM measurements

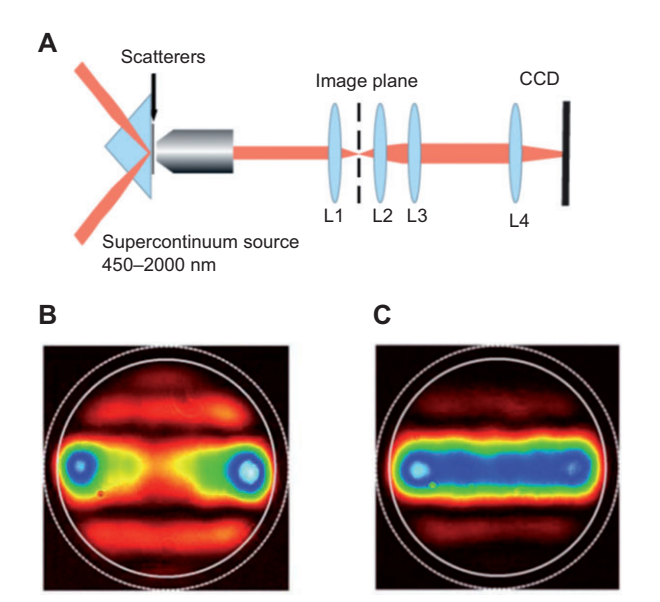


Figure 9 (A) Sketch of the experimental setup of a Fourier microscope. A high NA objective (NA=0.95) is combined with a set of telescope lenses L1 and L2, a Fourier lens L3, and a tube lens L4. (B) Fourier microscope image of a 2 µm long, 50 nm wide and 30 nm thick Au nanowire excited at 725 nm with p-polarized light with $200\,\mu\text{W}.$ (C) Same as in (B) but for s-polarized illumination of the nanowire. Reprinted with permission from Ref. [163], ©2011 by IOP Publishing LTD.

are different due to their ability to measure light fields close to the structures of interest by applying fiber optics and cantilevers to probe or disturb the light locally. In particular, the evanescent field close to the unit cells is accessible, in contrast to far-field techniques. It is difficult to give a general description of the resolution of the scanning optical microscope because of its working principle. Additionally, the light management – illumination and collection - follows different paths depending on each particular implementation. For instance the scattering SNOM collects light that is scattered to the far-field by disturbing the local fields with a tip. Collection of the scattered light can be done with conventional optical setups. In contrast, a fiber tip can be used as a SNOM probe to collect the light locally and the intensity that is collected with the fiber has to be analyzed. Approaches to illuminate with the fiber tip were also successfully demonstrated [169]. Often, the very small apertures of the collection optics (tapered optical fibers) lead to measurement systems with very low throughput and low signal to noise ratio. To obtain useful information contrasting enhancement techniques like cross polarization or attenuated total reflection geometries are implemented to separate the illumination and measurement path and increase sensitivity.

To provide an impression of the strength of the approach, we show here measurements of plasmonic resonant modes by a SNOM scattering technique. In this example, small plasmonic nanodisks were studied interferometrically. Cross polarization and second harmonic demodulation were applied as contrast enhancement techniques [170, 171]. The measurements impress by their ability to visualize different plasmonic modes for different nanodisks and deliver information of amplitude and phase, as demonstrated in Figure 10.

Whereas all previously discussed techniques have been using light as the carrier information, more elaborate schemes can be equally considered. This is possible by exciting resonances of plasmonic unit cells by other means than light such as, e.g., electrons. The origin of the plasmonic resonance is a displacement of electrons inside the unit cells and such a displacement can be induced, e.g., also directly with an electron beam. A recently introduced method to study the resonance behavior of single unit cells is the so-called electron energy loss spectroscopy

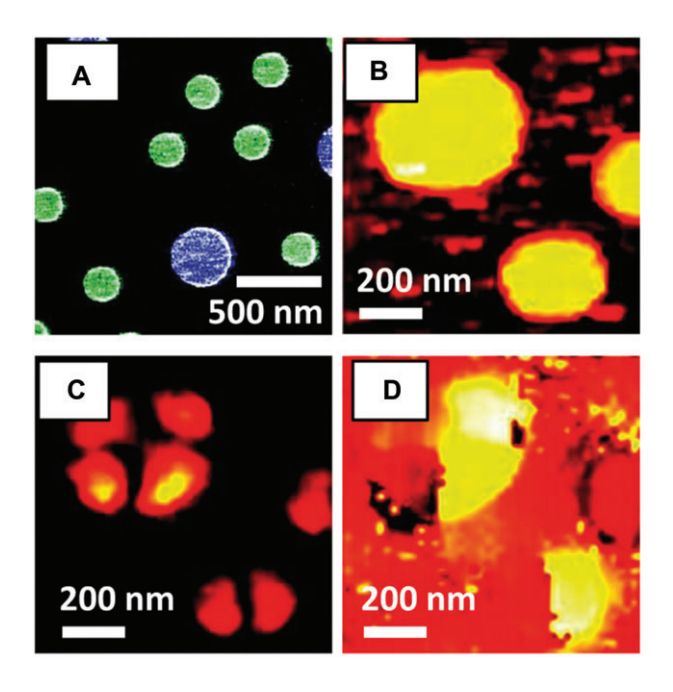


Figure 10 (A) False color SEM image of the investigated sample made of gold nanodisks of different radii. The recorded near-field optical image of an 1.1×1.1 μm² area contains only one large and two small nanodisks. (B) Topography, (C) optical amplitude, and (D) optical phase. Measurements were made at a wavelength of 875 nm. The illumination is at oblique incidence with the electric field polarization in the plane of the sample. The shown field component corresponds to the normal component of the electric field relative to the substrate. It can be seen that the smaller and the larger disk sustain plasmonic resonances of different modes. Reprinted with permission from Ref. [170], ©2008 by ACS.

(EELS). Using an electron beam for excitation allows the probing of different modes of plasmonic unit cells [172]. The method is fruitfully combined with electron microscopy [173] and delivers insights into the resonance behavior of unit cells through the possibility of local excitation [174].

Overall, various measurements and characterization techniques can be used to study self-assembled MMs at different spatial resolution levels. The specific aspects of the measurement setup and scheme such as angular spectra (or numerical aperture), angle of observation and type of measurement (specular or diffuse, etc.) need to be carefully considered to interpret the measurement results and supporting simulations usually have to be done. On the microscopic level, the resonances of single unit cells of MMs are studied to identify their resonances and to draw conclusions about behavior in an assembly, i.e., the entire MM.

6 Achievements, challenges, and applications

To put the work from previous chapters in a broader context, most notably also with respect to applications, it is worth stressing that a tremendous evolution has been witnessed in the past several years. The technological advancements made in the fabrication of structures have been strongly interlinked with novel suggestions from theory. Nonetheless, the advancements were bidirectional. It is not uniquely designs proposed by theoreticians which were picked up by experimentalists. On the contrary, with novel bottom-up nanofabrication techniques, geometries for structures became accessible which were previously not thought of. Overall we are currently at a point where many problems have been solved. However, of course, some of them still have to be mitigated.

The first achievement was to have materials available where metallic NPs are densely packed. This is essential to observe properties that are significantly different to those of isolated plasmonic NPs that have been known and used, though not understood, for over a thousand years. The second achievement was the development of a methodology to assemble MM unit cells from a larger number of plasmonic NPs into deterministic shapes. The nominal geometry of these unit cells is fairly identical, though the exact structure, i.e., the exact arrangement of NPs, varies among unit cells. Nonetheless, this is of less importance since the functionality is brought into the system by the nominal shape of the unit cell. However,

variations in the geometry also cause an inhomogeneous broadening of the resonances which is detrimental to a certain extent. Since the arrangement of unit cells relative to each other cannot be controlled in most cases (c.f. chapter 1), the unit cell itself is the remaining entity that carries the functionality and is thus merits discussion.

This also explains why the key properties discussed in this review, such as e.g., the magnetic dipole response, are usually at the focus of interest. The concentration on isolated unit cells and not on an ensemble thereof is also the focus in applications that were already implemented or at least suggested. A prominent example is the cloaking device [175] that allows the concealment of optically small objects. Details are shown in Figure 11. Although a usual three dimensional cloak for a macroscopic object requires a shell that is made from a material characterized by a suitable dispersive anisotropic permittivity and permeability [176], the constraints are relaxed for optically small scatterers, i.e., scatterers whose interaction with light can be treated as quasi-static [177]. Then, it was shown, that it is sufficient to cover the core object by a plasmonic shell to nullify the total scattering cross section. Here the purpose of the shell is to generate a scattered dipole field of the same strength as that generated by the core object but oscillating 180° out-of-phase. This causes destructive interference and a strongly reduced scattering; and eventually only a minor absorption of the incident energy in the core-shell particle. In more detail, the shell, for a given core object and a given shell thickness, has to attain a certain permittivity to provide a suitable scattering response. The real part of the permittivity can be either very negative or it may attain a value between zero and one. The imaginary part, obviously, should take values as small as possible. These properties can be met by the structures described in this review, e.g., the coreshell cluster as discussed in chapters 3 and 4. The shell made from silver NPs possesses effectively a Lorentzian dispersion around the effective plasmon resonance, as shown in Figure 11(E) [178]. At frequencies slightly larger than the resonance, the real part of the permittivity is very negative but absorption is high as well. This is detrimental for the cloaking effect. However, at larger frequencies where the real part of the permittivity is positive but yet smaller than unity, the second possible configuration is met and the shell can be used to suppress the scattering response [179]. This is clearly visible by looking at the scattering efficiencies [Figure 11(F)] or the field distributions of the core-shell cluster [Figure 11(D)]. Besides the advantage of having a cloak working at rather elevated frequencies; it turned out that the imaginary part of the composite is smaller than the intrinsic imaginary part of

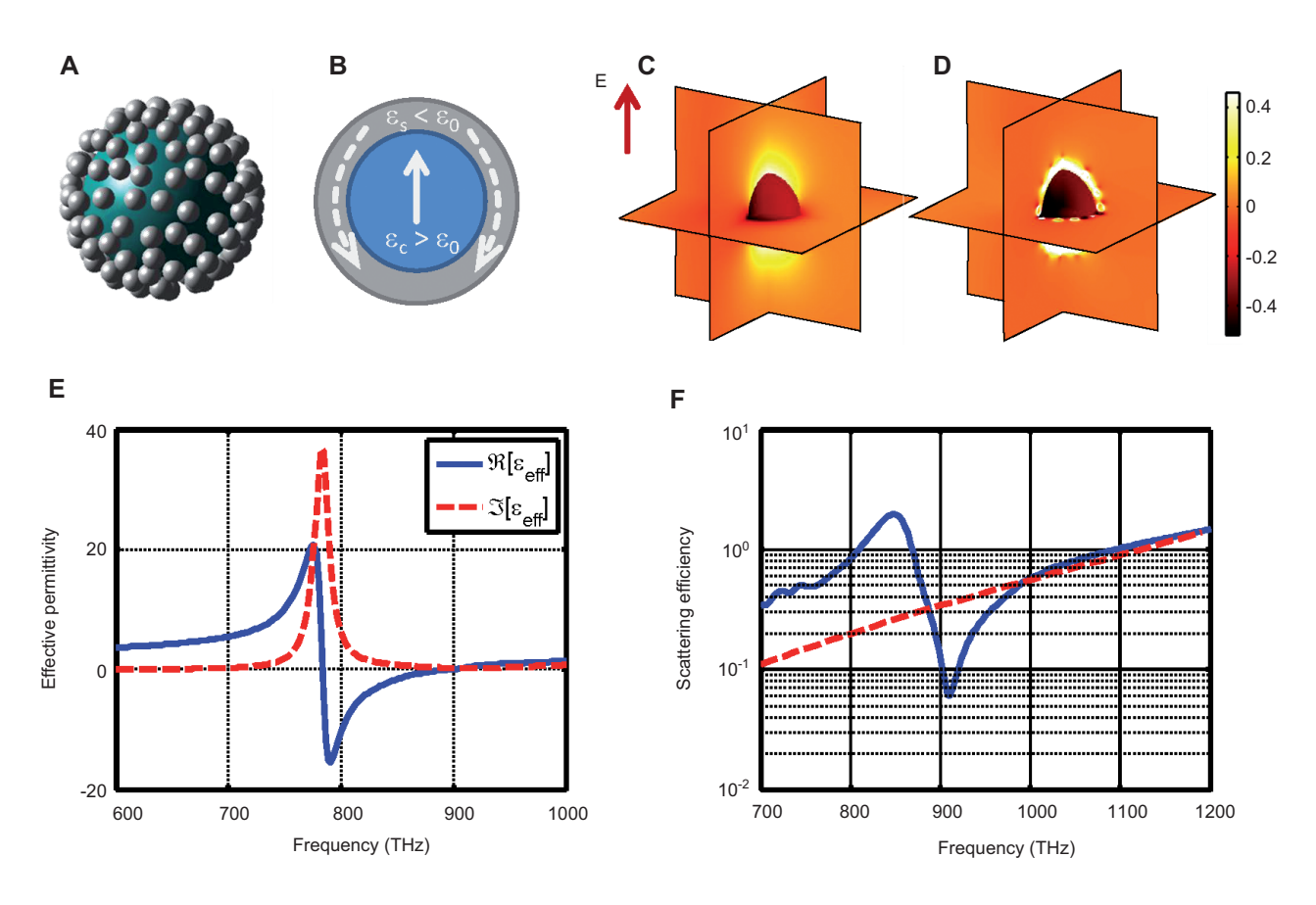


Figure 11 Demonstration of a self-assembled core-shell cluster working as a cloaking device. The cluster consists of a high permittivity core (radius=35 nm and ϵ =8) that is covered by silver NPs (radii=5 nm) forming a shell. (A) Schematic sketch of the core-shell cluster. (B) Illustration of the cloaking principle. The shell (made of amorphously arranged silver NPs) is assumed as homogeneous material [the dispersion of the effective permittivity is shown in (E)]. For values of the real part of the shell permittivity that are either negative or between zero and one the shell is able to cancel the polarization of the core. (C) Logarithmic plots of the electric field intensity at 910 THz for the bare core sphere. The clear excitation of an electric dipole response can be seen. (D) Same as in (C) but now for the core-shell cluster. The dipole radiation into the far-field is totally suppressed though some field enhancements in close vicinity to the shell appear due to the LSPRs in the silver NPs. (E) Effective permittivity of the silver NP shell. (F) Scattering efficiency as a function of the frequency for the dielectric core sphere (red-dashed curve) as well as for the core-shell cluster (blue-solid curve). An enormous reduction of the scattering of about 75% is visible at 910 THz.

the metal at the same frequency. This renders the shell made from plasmonic NPs to be a better shell material than the intrinsic metal. This is quite surprising and possible further applications may benefit from this improvement [180]. Refined versions of this cloak for cylindrical objects and extension to cloak larger objects, i.e., objects whose scattering response is dominated by the magnetic dipole, were also discussed [181, 182]. Such devices may not only find applications in cloaked sensors [183, 184] or in optical nanoantenna arrays with strongly suppressed cross-talk, but also in the reduction of the optical force on objects [185] or the cloaking of tips of near-field scanning optical microscopes [186].

Moreover, other key optical properties can be affected by unit cells made from an ensemble of just a few plasmonic NPs. A referential example is circular dichroism or, more general, chirality. Materials possessing such properties have been obtained by top-down nanofabrication technologies, but currently it remains elusive to have them available as bulk materials [187-194]. In contrast, comparable optical properties can be obtained if metallic NPs are assembled to form helical structures [195]. A large variety of methods can potentially be used but prominent methods consist of DNA- or peptide-directed assembly strategies such as DNA origami [52, 53]. Other direct optical properties that are at the focus of interest concern the effective anisotropy, i.e., the achievement of a large difference of the optical response depending on the orientation of the electric field relative to a preferential direction imposed by the sample [18]. There are generally two options to achieve such anisotropic response. The first is to use an intrinsic anisotropic environment such

as a liquid crystal into which metallic NPs can be embedded. In this case tunability can be achieved by changing the orientation of the liquid crystals in a cell by applying a voltage [196]. The overall response is anisotropic and depends on the molecular orientation. At elevated temperatures a phase change to an amorphous state may take place for the liquid crystal host material and the structure becomes isotropic. The second option is to use an anisotropic arrangement of a small number of metallic NPs as discussed in chapter 3 for the plasmonic dimer structure. There, it was stated that the polarizability of the ensemble depends on the orientation of the incident field relative to the orientation of the NP assembly. Eventually, it can be speculated that a combination of both strategies, embedding an anisotropic NP assembly into an anisotropic optical environment, can enhance the anisotropy even further.

However, although many of these applications and functionalities are extremely appealing and do indicate potential future directions of research, further problems remain to be solved. Potentially the biggest problem is to increase the as yet small filling fraction of plasmonic NPs. All possible effects would appear stronger since resonance strength and induced dispersion would be elevated. At the same time, care has to be taken that conductive coupling in the ensemble remains suppressed which would otherwise cause the appearance of novel plasmonic resonances [197]. They would emerge at frequencies far away from the frequency of the isolated NP in the assembly. Their contribution would essentially diminish the optical response. The suppression of a conductive coupling can be enforced, as outlined in the review, by means of electrostatic repulsion if all the NPs are left with a surface charge or by chemical means where the NPs are covered by some molecular shells. Eventually, it remains a technological problem to be solved to let NPs assemble as densely as possible while maintaining them optically isolated.

Another problem, which is frequently encountered while working towards MMs, is the choice of the appropriate size of the plasmonic NPs. This requires a careful balance. On the one hand, the particles should have a reasonable size for two reasons. First, smaller metallic particles suffer from a larger imaginary part in their intrinsic permittivity; reflecting an increased absorption due to increased collision of the free electrons with the boundaries of the NPs. Second, independent of the intrinsic material properties, absorption scales with the third power of the radius whereas scattering scales with the sixth power. This suggests that absorption dominates over scattering for very small particles and eventually any material appears black with no further functionality if made

from excessively small NPs. These considerations suggest that the plasmonic NPs should have a sufficient size. On the other hand, the actual unit cell from which the MM is made of shall be small or ideally much smaller when compared to the operating wavelengths. This prohibits the use of large plasmonic NPs in the construction of the unit cells. Both requirements conflict and a compromise has to be found which is sometimes unsatisfactory with respect to the functionality. A further problem that has to be mitigated is, as mentioned above, the inhomogeneous broadening of the observable resonances due to variations in geometry from unit cell to unit cell. Here chromatography can be used to isolate unit cells of certain properties but these technologies still need to be improved. Another problem is the preferential use of gold NPs in many devices for obvious reasons, i.e., most notably since it is chemically inert. Gold is known to have less preferable optical material properties when compared to silver, i.e., absorption is stronger at frequencies where the real part of the permittivity possesses suitable values. All of these problems cause an insufficient polarizability of the NP assemblies; independent of the number of NPs forming the assembly. Increasing this resonance strength can be understood as a primary challenge in future research.

One possible solution could be the use of NPs where only the shell is plasmonic. This suggests that the resonance frequency of individual NPs is shifted to longer wavelengths. Then, intrinsic absorption is reduced since the electric field no longer penetrates the volume of the plasmonic NP, the size constraints get relaxed, and gold becomes a more attractive material.

An alternative solution to increase the scattering strength is the incorporation of gain materials into the selfassembled structures [198]. This is possible by infiltrating the host material of the plasmonic NPs with fluorescent dyes (e.g., Rhodamine, Fluorescein), semiconductor quantum dots (e.g., InGaAs-GaAs quantum dots) or rare earth materials (e.g., erbium) [199, 200]. The approach is best illustrated by considering the resonance condition for a spherical plasmonic NP in the electric dipolar limit. Inspecting the denominator of the particle polarizability, it can be seen that a LSPR is sustained at the frequency ω when the condition $\varepsilon_{\text{Metal}}(\omega) + 2\varepsilon_{\text{Surrounding}}(\omega) = 0$ is met. However, the condition cannot be exactly met and the resonance frequency is shifted into the complex plane because of the finite imaginary part of the metal at the resonance frequency. If, however, the surrounding material is characterized by gain instead of absorption, suggesting that the imaginary part is negative instead of being positive, the resonance condition can be met exactly [201, 202]. Of course, this back-of-the-envelope calculation loses its validity the better the condition is met, but it provides a clear indication how a balanced and carefully tailored gain material can be designed to render all resonances sharper. It remains to be said that the perfect resonance leads to an unstable optical response with the onset of lasing or spasing that are difficult to predict [203, 204]. They can only be described using devoted numerical means that describe the gain material as a two or, even more realistically, as a four level system using a density matrix approach or at least using rate equations [205–207].

If these problems are solved we can safely expect a wealth of future applications well beyond those indicated previously in this review. A large number of applications were suggested for materials that possess a permittivity close to zero [208]. This property is also supported by materials made of densely packed plasmonic NPs. In resonance, where absorption is huge, operation is usually not suggested. But at the second crossing point, at higher frequencies, absorption is much lower and the material potentially allows propagation of electromagnetic fields over finite distances. Espilon-near-zero applications would also benefit from extremely sharp resonances. The further away the operation frequency is from the resonance the less severe absorption will be because the imaginary part of the permittivity decays with the third power of the frequency and the real part only with the second power. Since the wave in the epsilon-near-zero material does not have any phase advance, the geometrical surface of the epsilon-near-zero material imprints a spatial phase distribution on an incident plane wave [209]. This can be used to implement functional optical elements such as lenses, beamers, or spatial filters. Moreover, filling a waveguide bend with such material might permit perfect transmission; independent of the shape of the waveguides to be connected [210]. The implementation of applications that exploit the properties of a material made from densely packed plasmonic NPs is most likely to emerge in the near-future; since essentially the materials are already available.

Another application that has been suggested is that of a lens or even a perfect lens. This application can be thought of as an essential trigger of MM research [211]. Under the hypothetical assumption that a medium exists that possesses an isotropic negative permittivity as well as permeability at the same frequency, a slab made from such material can restore evanescent contributions of a source from an object plane before the slab in an image plane behind the slab. At its heart the slab sustains surface modes independent of the k-vector; hence all evanescent waves couple to the other side of the slab and the field does not decay in the MM. The imaging potential of the slab for propagating modes is best understood in terms of a diffraction coefficient, which is associated to the second derivative of the propagation constant with respect to the tangential wave vector [212]. In a material with the aforementioned properties, the diffraction coefficient is anomalous, i.e., it has an opposite sign when compared to the diffraction coefficient of free space. Having a sequence of propagations through free space and the perfect lens, the diffraction coefficient undergoes an alteration between normal and anomalous. Eventually, the overall diffraction is completely suppressed by choosing a suitable length for each section of the propagation [213]. The excitation of surface waves as well as the requirement of a suitable dispersion to cause anomalous diffraction was shown to be possible also for two separated slabs made from plasmonic NPs [214, 215].

Besides these applications that require a specific material, further applications exist that only require carefully tailored ensembles of plasmonic NPs. It is beyond the scope of this contribution to review all of them, but it remains to be mentioned that applications such as optical rulers [216], sensors [217], plasmonic substrates for surface enhanced Raman scattering [218], novel tools for spectroscopy that are sensitive to probe electric quadrupolar or magnetic dipolar transitions [136], solar cells [219], high density optical storage devices [220], or light emitting diodes [221] were all shown to profit from the incorporation of plasmonic NPs. We anticipate an exciting time in the near-future where eventually some of these applications are not only explored in academia but may find their way into real-world products.

After presenting this long list of applications of bottom-up MMs we want to compare once again their advantages and disadvantages to conventional topdown MMs. This should allow putting the given aspects of this review into a broader context. As already indicated, top-down MMs are usually fabricated by lithographic processes or direct writing such as focused electron- or ion-beam lithography. Therefore, the MMs are built-up by writing each single unit cell onto a substrate. One advantage is that highly periodic structures can be achieved, or in other words, the long-range order between the unit-cells can be controlled at will. Contrariwise, top-down techniques normally work on a substrate and three-dimensional structures can only be realized by stacking of different layers [222], which remains a complicated task. Furthermore, since every unit cell is written sequentially, top-down processes are normally too slow to fabricate large-scale samples of macroscopic dimension. These two issues of achieving bulky MMs with macroscopic dimension can be solved by relying

on bottom-up techniques. As intensively discussed in chapters 1 and 4 most of the bottom-up techniques work in solution and therefore they are three-dimensional by definition. The evoked self-assembly takes place everywhere in the solution, i.e., contrary to top-down techniques all unit cells are fabricated in parallel making the fabrication of large-scale samples incredibly fast. Up to now, in most cases the long-range order between the unit cells cannot be controlled by bottom-up fabrication techniques resulting in an amorphous arrangement. The consequences thereof were discussed in detail in chapter 2 and 3. Another crucial advantage of bottom-up techniques is the control of distances or more physically the resolution limit of the fabrication process. Whereas for top-down techniques the minimal structure size is given by the spot size of, e.g., the electron beam (around 20 nm) for bottom-up techniques such limitations do not exist, since in most cases it depends on the length of the linker molecules attached to the NPs. Typical separations down to 1 nm [59, 62] are reported and even sub-nm separations have been achieved [223].

7 Conclusions

To concisely conclude, we have been reviewing the stateof-the-art of the theoretical description, the nanofabrication, and the optical characterization of self-assembled plasmonic nanostructures. The starting point of these materials is a plasmonic NP that sustains a strong interaction of light at the frequency where a localized surface plasmon polariton is excited. To achieve, however, a scattering response that is beyond what is possible with an isolated plasmonic NP, mechanisms have to be exploited that allow the self-assembly of a larger number of plasmonic NPs into functional unit cells. These unit cells are fabricated by bottom-up techniques established in nanochemistry. Although a nominal geometry of a unit cell can be fabricated at high precision, its exact geometry and the arrangement of a larger number of unit cells relative to each other is usually less controllable. This implies major challenges for the theoretical description and the understanding of the functionality and the optical action of MMs made from such unit cells.

Nevertheless, much progress has been made and a clear path towards future development has been identified. Theoretically, a technique has been reviewed here that expands the scattered field of an arbitrary complicated unit cell into contributions of Cartesian multipoles. This allows the simplification of the theoretical

description of the optical response of individual unit cells while considering only a few leading multipole coefficients in any further description. It is worth stressing that this is especially important in the field of MMs where effective properties can be assigned to a medium made of unit cells whose scattering response is dominated by an electric and a magnetic dipole only. Moreover, the expansion of the scattering response into multipoles provides a clear language in which the functionality of the unit cells can be discussed. It has also been presented what unit cells of interest look like and what exactly makes them attractive. Although, a functional element can be already made from two NPs, an entire new class of structures becomes accessible based on the collective response of a cluster of a large number of plasmonic NPs in close proximity. The respective geometries can be, e.g., spheres or shells which possess a scattering response that is dominated by a magnetic dipole. How these unit cells can be fabricated and how they can be characterized was equally reviewed in detail. Primary applications have been indicated along with challenges that have to be met to assure a further progress of the entire field.

Overall it has to be stressed that only a finite fraction of the prosperous field has been reviewed in this contribution. Many aspects were, moreover, only touched upon. This entire field of research where chemistry, material science, photonics and optics are fused is quickly evolving. The interdisciplinary character firmly invites researchers with a complimentary expertise to contribute to this field with suggestions for novel theoretical means, fabrication techniques, or characterization methodologies to identify solutions for urgent problems and unprecedented applications.

Far reaching goals for future work are the general control of electromagnetic fields on the nanoscale where self-assembled plasmonic entities are used to steer the light and its interaction with adjacent nanometric objects. A liquid negative index metamaterial might be an appealing structure but self-assembled optical nanoantennas that can efficiently extract and direct light from single photon sources might be equally referential future applications. With these achievements, optics in general and nanophotonics specifically would be once again an enabler for many applications in the field of optical signal processing, in distant sensing devices, ultrafast nonlinear spectroscopy, photocatalysis, and solar cells.

Acknowledgments: The authors would like to thank S.A. Tretyakov, C.R. Simovski, M. Nieto-Vesperinas, and A.F. Koenderink for fruitful discussions. Financial support by the Federal Ministry of Education and Research PHONA, from the State of Thuringia within the ProExcellence program MEMA, as well as from the European Union FP7 project NANOGOLD is acknowledged. The authors would like to thank all the partners from the NANOGOLD project for the stimulating atmosphere and the many enlightening discussions about self-assembled plasmonic nanostructures.

Received November 9, 2012; accepted March 7, 2013; previously published online April 4, 2013

References

- [1] Alivisatos AP, Johnsson KP, Peng X, Wilson TE, Loweth CJ, Bruchez Jr. MP, Schultz PG. Organization of 'nanocrystal molecules' using DNA. Nature 1996;382:609-11.
- [2] Brousseau III LC, Novak JP, Marinakos SM, Feldheim DL. Assembly of phenylacetylene-bridged gold nanocluster dimers and trimers. Adv Mater 1999;11:447-9.
- [3] Bishop KJM, Wilmer CE, Soh S, Grzybowski BA. Nanoscale forces and their uses in self-assembly. Small 2009;5:1600-30.
- [4] Choi CL, Alivisatos AP. From artificial atoms to nanocrystal molecules: preparation and properties of more complex nanostructures. Annu Rev Phys Chem 2010;61:369-89.
- [5] Romo-Herrera JM, Alvarez-Puebla RA, Liz-Marzan LM. Controlled assembly of plasmonic colloidal nanoparticle clusters. Nanoscale 2011;3:1304-15.
- [6] Guerrero-Martinez A, Alonso-Gomez JL, Auguie B, Cid MM, Liz-Marzan LM. From individual to collective chirality in metal nanoparticles. Nano Today 2011;6:381-400.
- [7] Cheng JY, Ross CA, Thomas EL, Smith HI, Vancso GJ. Fabrication of nanostructures with long-range order using block copolymer lithography. Appl Phys Lett 2002;81:3657-9.
- [8] Darling SB. Directing the self-assembly of block copolymers. Proc Polym Sci 2007;32:1152-204.
- [9] Smart T, Lomas H, Massignani M, Flores-Merino MV, Perez LR, Battaglia G. Block copolymer nanostructures. Nano Today 2008;3:38-46.
- [10] Bang J, Jeong U, Ryu DY, Russell TP, Hawker CJ. Block copolymer nanolithography: translation of molecular level control to nanoscale patterns. Adv Mater 2009;21:4769-92.
- [11] Polleux J, Rasp M, Louban J, Plath N, Feldhoff A, Spatz JP. Benzyl alcohol and block copolymer micellar lithography: a versatile route to assembling gold and in situ generated titania nanoparticles into uniform binary nanoarrays. ACS Nano 2011;5:6355-64.
- [12] Vignolini S, Yufa NA, Cunha PS, Guldin S, Rushkin I, Stefik M, Hur K, Wiesner U, Baumberg JJ, Steiner U. A 3D optical metamaterial made by self-assembly. Adv Mater 2012;24:OP23-7.
- [13] Wang X, Kwon DH, Werner DH, Khoo I-C, Kildishev AV, Shalaev VM. Tunable optical negative-index metamaterials employing anisotropic liquid crystals. Appl Phys Lett 2007;91:143122.
- [14] Pratibha R, Park K, Smalyukh II, Park W. Tunable optical metamaterial based on liquid crystal-gold nanosphere composite. Opt Express 2009;17:19459-69.
- [15] Pratibha R, Park W, Smalyukh II. Colloidal gold nanosphere dispersions in smectic liquid crystals and thin nanoparticledecorated smectic films. J Appl Phys 2010;107:063511.
- [16] Zappone B, Lacaze E, Hayeb H, Goldmann M, Boudet N, Barois P, Alba M. Self-ordered arrays of linear defects and virtual singularities in thin smectic-A films. Soft Mater 2011; 7:1161-7.

- [17] Dintinger J, Tang B-J, Zeng X, Liu F, Kienzler T, Mehl GH, Ungar G, Rockstuhl C, Scharf T. A Self-organized anisotropic liquid-crystal plasmonic metamaterial. Adv Mater 2013, DOI: 10.1002/adma.201203965.
- [18] Zeng X, Liu F, Fowler AG, Ungar G, Cseh L, Mehl GH, Macdonald JE. 3D ordered gold strings by coating nanoparticles with mesogens. Adv Mater 2009;21:1746-50.
- [19] Macfarlane RJ, Lee B, Jones MR, Harris N, Schatz GC, Mirkin CA. Nanoparticle superlattice engineering with DNA. Science 2011;
- [20] Cheng W, Campolongo MJ, Cha JJ, Tan SJ, Umbach CC, Muller DA, Luo D. Free-standing nanoparticle superlattice sheets controlled by DNA. Nature Mater 2009;8:519-25.
- [21] Hung AM, Micheel CM, Bozano LD, Osterbur LW, Wallraff GM, Cha JN. Large-area spatially ordered arrays of gold nanoparticles directed by lithographically confined DNA origami. Nature Nanotech 2010;5:121-6.
- [22] Chen Y, Fu J, Ng KC, Tang Y, Cheng W. Free-standing polymer nanoparticle superlattice sheets self-assembled at the air liquid interface. Cryst Growth Des 2011;11:4742-6.
- [23] Ng KC, Udagedara IB, Rukhlenko ID, Chen Y, Tang Y, Premaratne M, Cheng W. Free-standing plasmonic-nanorod superlattice sheets. ACS Nano 2012;6:925-34.
- [24] Wen T, Majetich SA. Ultra-large-area self-assembled monolayers of nanoparticles. ACS Nano 2011;5:8868-76.
- [25] Stebe KJ, Lewandowski E, Ghosh M. Oriented assembly of metamaterials. Science 2009;325:159-60.
- [26] Tamma VA, Lee J-H, Wu Q, Park W. Visible frequency magnetic activity in silver nanocluster metamaterial. Appl Opt 2010;49:A11-7.
- [27] Lee JH, Wu Q, Park W. Metal nanocluster metamaterial fabricated by the colloidal self-assembly. Opt Lett 2009;34:443-5.
- [28] Lerond T, Proust J, Yockell-Lelievre H, Gerard D, Plain J. Self-assembly of metallic nanoparticles into plasmonic rings. Appl Phys Lett 2011;99:123110.
- [29] Cui Y, Björk MT, Liddle JA, Sönnichsen C, Boussert B, Alivisatos AP. Integration of colloidal nanocrystals into lithographically patterned devices. Nano Lett 2004;4:1093-8.
- [30] Kraus T, Malaquin L, Schmid H, Riess W, Spencer ND, Wolf H. Nanoparticle printing with single-particles resolution. Nature Nanotech 2007;2:570-6.
- [31] Fan JA, Bao K, Sun L, Bao J, Manoharan VN, Nordlander P, Capasso F. Plasmonic mode engineering with templated self-assembled nanoclusters. Nano Lett 2012;12; 5381-24.
- [32] Henzie J, Grünwald M, Widmer-Cooper A, Geissler PL, Yang P. Self-assembly of uniform polyhedral silver nanocrystals into densest packings and exotic superlattices. Nature Mater 2012;11:131-7.

- [33] Tao AR, Ceperley DP, Sinsermsuksakul P, Neureuther AR, Yang P. Self-organized silver nanoparticles for three-dimensional plasmonic crystals. Nano Lett 2008;8:4033-8.
- [34] Talapin DV, Shevchenko EV, Bodnarchuk MI, Ye X, Cheng J, Murray CB. Quasicrystalline order in self-assembled binary nanoparticle superlattices. Nature 2009;461:964-7.
- [35] Fan JA, Wu C, Bao K, Bao J, Bardhan R, Halas NJ, Manoharan VN, Nordlander P, Shvets G, Capasso F. Self-assembled plasmonic nanoparticle clusters. Science 2010;328:1135-8.
- [36] Chuntonov L, Haran G. Trimeric plasmonic molecules: the role of symmetry. Nano Lett 2011;11:2440-5.
- [37] Fan JA, Bao K, Wu C, Bao J, Bardhan R, Halas NJ, Manoharan VN, Shvets G, Nordlander P, Capasso F. Fano-like interference in self-assembled plasmonic quadrumer clusters. Nano Lett 2010:10:4680-5.
- [38] Tan SJ, Campolongo MJ, Luo D, Cheng W. Building plasmonic nanostructures with DNA. Nature Nanotech 2011;6:268-76.
- [39] Mirkin CA, Letsinger RL, Mucic RC, Storhoff JJ. A DNA-based method for rationally assembling nanoparticles into macroscopic materials. Nature 1996;382:607-9.
- [40] Wilner OI, Willner I. Functionalized DNA nanostructures. Chem Rev 2012;112:2528-56.
- [41] Watanabe-Tamaki R, Ishikawa A, Tanaka T, Zako T, Maeda M. DNA-templating mass production of gold trimer rings for optical metamaterials. J Phys Chem C 2012;116:15028-33.
- [42] Claridge SA, Goh SL, Frechet JMJ, Williams SC, Micheel CM, Alivisatos AP. Directed assembly of discrete gold nanoparticle groupings using branched DNA scaffolds. Chem Mater 2005;17:1628-35.
- [43] Soto CM, Srinivasan A, Ratna BR. Controlled assembly of mesoscale structures using DNA as molecular bridges. J Am Chem Soc 2002;124:8508-9.
- [44] Sheikholeslami S, Jun YW, Jain PK, Alivisatos AP. Coupling of optical resonances in a compositionally asymmetric plasmonic nanoparticle dimer. Nano Lett 2010;10:2655-60.
- [45] Fan JA, He Y, Bao K, Wu C, Bao J, Schade NB, Manoharan VN, Shvets G, Nordlander P, Liu DR, Capasso F. DNA-enabled self-assembly of plasmonic nanoclusters. Nano Lett 2011;11:4859-64.
- [46] Barrow SJ, Funston AM, Gomez DE, Davis TJ, Mulvaney P. Surface plasmon resonances in strongly coupled gold nanosphere chains from monomer to hexamer. Nano Lett 2011;11:4180-7.
- [47] Xing H, Wang Z, Xu Z, Wong NY, Xiang Y, Liu GL, Lu Y. DNA-directed assembly of asymmetric nanoclusters using Janus nanoparticles. ACS Nano 2012;6:802-9.
- [48] Nykypanchuk D, Maye MM, van der Lelie D, Gang O. DNA-guided crystallization of colloidal nanoparticles. Nature 2008;451:549-52.
- [49] Mastroianni AJ, Claridge SA, Alivisatos AP. Pyramidal and chiral groupings of gold nanocrystals assembled using DNA scaffolds. J Am Chem Soc 2009;131:8455-9.
- [50] Sharma S, Chhabra R, Cheng A, Brownell J, Liu Y, Yan H. Controll of self-assembly of DNA tubules through integration of gold nanoparticles. Science 2009;323:112-6.
- [51] Rothemund PWK. Folding DNA to create nanosclae shapes and patterns. Nature 2006;440:297-302.
- [52] Shen X, Song C, Wang J, Shi D, Wang Z, Liu N, Ding B. Rolling up gold nanoparticle-dressed DNA origami into threedimensional plasmonic chiral nanostructures. J Am Chem Soc 2012;134:164-49.

- [53] Kuzyk A, Schreiber R, Fan Z, Pradatscher G, Roller EM, Högele A, Simmel FC, Govorov AO, Liedl T. DNA-based self-assembly of chiral plasmonic nanostructures with tailored optical response. Nature 2012;483:311-4.
- [54] Novak JP, Feldheim DL. Assembly of phenylacetylenebridged silver and gold nanoparticle arrays. J Am Chem Soc 2000;122:3979-80.
- [55] Mühlig S, Rockstuhl C, Yannopapas V, Bürgi T, Shalkevich N, Lederer F. Optical properties of a fabricated self-assembled bottom-up bulk metamaterial. Opt Express 2011;19:9607-16.
- [56] Shalkevich N, Shalkevich A, Si-Ahmed L, Bürgi T. Reversible formation of gold nanoparticle-surfactant composite assemblies for the preparation of concentrated colloidal solutions. Phys Chem Chem Phys 2009;11:10175-9.
- [57] Dintinger J, Mühlig S, Rockstuhl C, Scharf T. A bottom-up approach to fabricate optical metamaterials by self-assembled metallic nanoparticles. Opt Mater Express 2012;2:269-78.
- [58] Walker DA, Kowalczyk B, de la Cruz MO, Grzybowski BA. Electrostatics at the nanoscale. Nanoscale 2011;3:1316-44.
- [59] Cunningham A, Mühlig S, Rockstuhl C, Bürgi T. Coupling of plasmon resonances in tunable layered arrays of gold nanoparticles. J Phys Chem C 2011;115:8955-60.
- [60] Brown LV, Sobhani H, Lassiter JB, Nordlander P, Halas NJ. Heterodimers: plasmonic properties of mismatched nanoparticle pairs. ACS Nano 2010;4:819-32.
- [61] Hyder MN, Lee SW, Cebeci FC, Schmidt DJ, Shao-Horn Y, Hammond PT. Layer-by-layer assembled polyaniline nanofiber/ multiwall carbon nanotube thin film electrodes for high-power and high-energy storage applications. ACS Nano 2011;5: 8552-61.
- [62] Cunningham A, Mühlig S, Rockstuhl C, Bürgi T. Exciting bright and dark eigenmodes in strongly coupled asymmetric metallic nanoparticle arrays. J Phys Chem C 2012;116:17746-52.
- [63] Mühlig S, Cunningham A, Scheeler S, Pacholski C, Bürgi T, Rockstuhl C, Lederer F. Self-assembled plasmonic core-shell clusters with an isotropic magnetic dipole response in the visible range. ACS Nano 2011;5:6586-92.
- [64] Gellner M, Niebling S, Kuschelmeister HY, Schmuck C, Schlücker S. Plasmonically active micron-sized beads for integrated solid-phase synthesis and label-free SERS analysis. Chem Comm 2011;47:12762-4.
- [65] Gellner M, Steinigeweg D, Ichilman S, Salehi M, Schütz M, Kömpe K, Haase M, Schlücker S. 3D self-assembled plasmonic superstructures of gold nanospheres: synthesis and characterization at the single-particle level. Small 2011;7:3445-51.
- [66] Hong Y, Pourmand M, Boriskina SV, Reinhard BM. Enhanced light focusing in self-assembled optoplasmonic clusters with subwavelength dimensions. Adv Mater 2012;25:115-9.
- [67] Pawlak DA, Turczynski S, Gajc M, Kolodziejak K, Diduszko R, Rozniatowski K, Smalc J, Vendik I. How far are we from making metamaterials by self-organization? The microstructure of highly anisotropic particles with an SRR-like geometry. Adv Func Mater 2010;20:1116-24.
- [68] Reyes-Coronado A, Acosra MF, Merino RI, Orera VM, Kenanakis G, Katsarakis N, Kafesaki M, Mavidis C, Garcia de Abajo J, Economou EN, Soukoulis CM. Self-organization approach for THz polaritonic metamaterials. Opt Express 2012;20:14663-82.
- [69] Senyuk B, Evans JS, Ackerman PJ, Lee T, Manna P, Vigderman L, Zubarev ER, van de Lagemaat J, Smalyukh II. Shape-dependent

- oriented trapping and scaffolding of plasmonic nanoparticles by topological defects for self-assembly of colloidal dimers in liquid crystals. Nano Lett 2012;12:955-63.
- [70] Menzel C, Paul T, Rockstuhl C, Pertsch T, Tretyakov S, Lederer F. Validity of effective material parameters for optical fishnet metamaterials. Phys Rev B 2010;81:035320.
- [71] Albooyeh M, Morits D, Tretyakov SA. Effective electric and magnetic properties of metasurfaces in transition from crystalline to amorphous state. Phys Rev B 2012;85:205110.
- [72] Tretyakov S. Applied electromagnetics. Norwood, MA: Artech House, INC.; 2003.
- [73] Helgert C, Rockstuhl C, Etrich C, Menzel C, Kley E-B, Tünnermann A, Lederer F, Pertsch T. Effective properties of amorphous metamaterials. Phys Rev B 2009;79:233107.
- [74] Rockstuhl C. Menzel C. Mühlig S. Petschulat I. Helgert C. Etrich C, Chipouline A, Pertsch T, Lederer F. Scattering properties of meta-atoms. Phys Rev B 2011;83:245119.
- [75] Pendry JB, Holden AJ, Robbins DJ, Stewart WJ. Magnetism from conductors and enhanced nonlinear phenomena. IEEE Trans Microwave Theory Tech 1999;47:2075-84.
- [76] Linden S, Enkrich C, Wegener M, Zhou J, Koschny T, Soukoulis CM. Magnetic response of metamaterials at 100 terahertz. Science 2004;306:1351-3.
- [77] Sersic I, Frimmer M, Verhagen E, Koenderink AF. Electric and magnetic dipole coupling in near-infrared split-ring metamaterial arrays. Phys Rev Lett 2009;103:213902.
- [78] Sersic I, Tuambilangana C, Kampfrath T, Koenderink AF. Magnetoelectric point scattering theory for metamaterial scatterers. Phys Rev B 2011;83:245102.
- [79] Petschulat J, Menzel C, Chipouline A, Rockstuhl C, Tünnermann A, Lederer F, Pertsch T. Multipole approach to metamaterials. Phys Rev A 2008;78:043811.
- [80] Rockstuhl C, Lederer F, Etrich C, Zentgraf T, Kuhl J, Giessen H. On the reinterpretation of resonances in split-ring-resonators at normal incidence. Opt Express 2006;14:8827-36.
- [81] Corrigan TD, Kolb PW, Sushkov AB, Drew HD, Schmadel DC, Phaneuf RJ. Optical plasmonic resonances in split-ring resonator structures: an improved LC model. Opt Express 2008;16:19850-64.
- [82] Waterman PC. Symmetry, unitarity, and geometry in electromagnetic scattering. Phys Rev D 1971;3:825-39.
- [83] Mishchenko MI, Travis LD, Mackowski DW. T-matrix computations of light scattering by nonspherical particles: a review. J Quant Spectrosc Radiat Transfer 1996;55:535-75.
- [84] Nieminen TA, Heckenberg NR, Rubinsztein-Dunlop H. Computational modeling of optical tweezers. In: Dholakia K, ed. Spalding GC, 2nd ed. (SPIE) Conference Series 2004;5514:514-23.
- [85] Mackowski DW, Mishchenko MI. Calculation of the T matrix and the scattering matrix for ensembles of spheres. J Opt Soc Am A 1996;13:2266-78.
- [86] Schneider JB, Peden IC. Differential cross section of a dielectric ellipsoid by the T-matrix extended boundary condition method. IEEE Trans Antennas Propag 1988;36:1317-21.
- [87] Nieminen TA, Loka VLY, Stilgoe AB, Knöner G, Branczyk AM, Heckenberg NR, Rubinsztein-Dunlop H. Optical tweezers computational toolbox. J Opt A: Pure Appl Opt 2007;9: 196-203.
- [88] Mühlig S, Menzel C, Rockstuhl C, Lederer F. Multipole analysis of meta-atoms. Metamaterials 2011:5:64-73.

- [89] Xu Y. Electromagnetic scattering by an aggregate of spheres. Appl Opt 1995;34:4573-88.
- [90] Mühlig S, Rockstuhl C, Pniewski J, Simovski CR, Tretyakov SA, Lederer F. Three-dimensional metamaterial nanotips. Phys Rev B 2010;81:075317.
- [91] Bohren CF, Huffman DR. Absorption and scattering of light by small particles. Weinheim, Germany: Wiley-VCH Verlag GmbH & Co. KgaA; 2004.
- [92] Choy TC. Effective medium theory: principles and applications. New York, USA: Oxford University Press; 1999.
- [93] Sihvola A. Electromagnetic mixing formulas and applications. London, UK: The Institution of Electrical Engineers; 1999.
- [94] Grahn P, Shevchenko A, Kaivola M. Electromagnetic multipole theory for optical nanomaterials. New J Phys 2012;14:093033.
- [95] Palik ED. Handbook of optical constants and solids. Orlando. USA: Acedemic Press; 1985.
- [96] Evlyukhin AB, Reinhardt C, Seidel A, Luk'yanchuk BS, Chichkov BN. Optical response features of Si-nanoparticle arrays. Phys Rev B 2010;82;045404.
- [97] Garcia-Etxarri A, Gomez-Medina R, Froufe-Perez LS, Lopez C, Chantada L, Scheffold F, Aizpurua J, Nieto-Vesperinas M, Saenz JJ. Strong magnetic response of submicron silicon particles in the infrared. Opt Express 2011;19:4815-26.
- [98] Zhao Q, Zhou J, Zhang F, Lippens D. Mie resonance-based dielectric metamaterials. Mater Today 2009;12:60-9.
- [99] Yannopapas V, Moroz A. Negative refractive index metamaterials from inherently non-magnetic materials for deep infrared to terahertz frequency ranges. J Phys Condens Mater 2005;17:3717-34.
- [100] Wheeler MS, Aitchison JS, Mojahedi M. Three-dimensional array of dielectric spheres with an isotropic negative permeability at infrared frequencies. Phys Rev B 2005;72:193103.
- [101] Seo BJ, Ueda T, Itoh T, Fetterman H. Isotropic left handed material at optical frequency with dielectric spheres embedded in negative permittivity medium. Appl Phys Lett 2006;88:161122.
- [102] Jylhä L, Kolmakov I, Maslovski S, Tretyakov S. Modeling of isotropic backward-wave materials composed of resonant spheres. J Appl Phys 2006;99:043102.
- [103] Yannopapas V. Negative refraction in random photonic alloys of polaritonic and plasmonic microspheres. Phys Rev B 2007;75:035112.
- [104] Yannopapas V. Artificial magnetism and negative refractive index in three-dimensional metamaterials of spherical particles at near-infrared and visible frequencies. Appl Phys A 2007;87:259-64.
- [105] Schuller JA, Zia R, Taubner T, Brongersma ML. Dielectric metamaterials based on electric and magnetic resonances of silicon carbide particles. Phys Rev Lett 2007;99:107401.
- [106] Wheeler MS, Aitchison JS, Chen JIL, Ozin GA, Mojahedi M. Infrared magnetic response in a random silicon carbide micropowder. Phys Rev B 2009;79:073103.
- [107] Evlyukhin AB, Novikov SM, Zywietz U, Eriksen RL, Reinhard C, Bozhevolnyi SI, Chichkov BN. Demonstration of magnetic dipole resonances of dielectric nanospheres in the visible region. Nano Lett 2012;12:3749-55.
- [108] Kuznetsov Al, Miroshnichenko AE, Fu YH, Zhang J, Luk'yanchuk B. Magnetic light. Nature Sci Report 2012;2:492.

- [109] Nordlander P, Oubre C, Prodan E, Li K, Stockman MI. Plasmon hybridization in nanoparticle dimers. Nano Lett 2004;4:899-903.
- [110] Riikonen S, Romero I, Garcia de Abajo FJ. Plasmon tunability in metallodielectric metamaterials. Phys Rev B 2005;71:235104.
- [111] Grahn P, Shevchenko A, Kaivola M. Electric dipole-free interaction of visible light with pairs of subwavelength-size silver particles. Phys Rev B 2012:86:035419.
- [112] Rockstuhl C, Lederer F, Etrich C, Pertsch T, Scharf T. Design of an artificial three-dimensional composite metamaterial with magnetic resonances in the visible range of the electromagnetic spectrum. Phys Rev Lett 2007;99:017401.
- [113] Simovski CR, Tretyakov SA. Model of isotropic resonant magnetism in the visible range based on core-shell clusters. Phys Rev B 2009;79:045111.
- [114] Vallecchi A, Albani M, Capolino F. Collective electric and magnetic plasmonic resonances in spherical nanoclsuters. Opt Express 2011;19:2754-72.
- [115] Urzhumov YA, Shvets G, Fan JA, Capasso F, Brandl D, Nordlander P. Plasmonic nanoclusters: a path towards negative-index metafluids. Opt Express 2007;15: 14129-45.
- [116] Alu A, Salandrino A, Engheta N. Negative effective permeability and left-handed materials at optical frequencies. Opt Express 2006;14:1557-67.
- [117] Alu A, Engheta N. The quest for magnetic plasmons at optical frequencies. Opt Express 2009;17:5723-30.
- [118] Barrow SJ, Wei X, Baldauf JS, Funston AM, Maulvaney P. The surface plasmon modes of self-assembled gold nanocrystals. Nature Commun 2012;3:1275.
- [119] Halas NJ, Lal S, Chang WS, Link S, Nordlander P. Plasmons in strongly coupled metallic nanostructures. Chem Rev 2011;111:3913-61.
- [120] Halas NJ, Plasmonics: an emerging field fostered by Nano Letters. Nano Lett 2010;10:3816-22.
- [121] Enustun BV, Turkevich J. Coagulation of colloidal gold. J Am Chem Soc 1963;85:3317-28.
- [122] Kimling J, Maier M, Okenve B, Kotaidis V, Ballot H, Plech A. Turkevich method for gold nanoparticle synthesis revisited. J Phys Chem B 2006;110:15700-7.
- [123] Lee PC, Meisel D. Adsorption and surface-enhanced raman of dyes on silver and gold sols. J Phys Chem 1982;86:3391-5.
- [124] Goulet PJG, Lennox RB. New insights into Brust-Schiffrin metal nanoparticle synthesis. J Am Chem Soc 2010;132:9582-4.
- [125] Perez-Juste J, Pastoriza-Santos I, Liz-Marzan LM, Mulvaney P. Gold nanorods: synthesis, characterization and applications. Coord Chem Rev 2005;249:1870-901.
- [126] Qi H, Lepp A, Heiney PA, Hegmann T. Effects of hydrophilic and hydrophobic gold nanoclusters on the stability and ordering of bolaamphiphilic liquid crystals. J Mater Chem 2007;17:2139-44.
- [127] Chen C-L, Zhang P, Rosi NL. A new peptide-based method for the design and synthesis of nanoparticle superstructures: construction of highly ordered gold nanoparticle double helices. J Am Chem Soc 2008;130:13555-7.
- [128] Shevchenko EV, Talapin DV, Kotov NA, O'Brien S, Murray CB. Structural diversity in binary nanoparticle superlattices. Nature 2006;439:55-9.

- [129] Nie Z, Fava D, Rubinstein M, Kumacheva E. "Supramolecular" assembly of gold nanorods end-terminated with polymer "pom-poms": effect of pom-pom structure on the association modes. J Am Chem Soc 2008;130:3683-9.
- [130] Lim D-k, Jeon K-S, Kim HM, Nam J-M, Suh YD. Nanogap-engineerable Raman-active nanodumbbells for single-molecule detection. Nature Mater 2010;9:60-7.
- [131] Kühn S, Hakanson U, Rogobete L, Sandoghdar V. Enhancement of single-molecule fluorescence using a gold nanoparticle as an optical nanoantenna. Phys Rev Lett 2006;97:017402.
- [132] Bharadwaj P, Deutsch B, Novotny L. Optical antennas. Adv Opt Photon 2009;1;438-83.
- [133] Kinkhabwala A, Yu Z, Fan S, Avlasevich Y, Müllen K, Moerner WE. Large single-molecule fluorescence enhancements produced by a bowtie nanoantenna. Nature Photon 2009;3:654-57.
- [134] Curto AG, Volpe G, Taminiau TH, Kreuzer MP, Quidant R, van Hulst NF. Unidirectional emission of a quantum dot coupled to a nanoantenna. Science 2010;329:930-3.
- [135] Esteban R, Teperik TV, Greffet JJ. Optical patch antennas for single photon emission using surface plasmon resonances. Phys Rev Lett 2010;104:026802.
- [136] Filter F, Mühlig S, Eichelkraut T, Rockstuhl C, Lederer F. Controlling the dynamics of quantum mechanical systems sustaining dipole-forbidden transitions via optical nanoantennas. Phys Rev B 2012;86:035404.
- [137] Kern AM, Martin OJF. Strong enhancement of forbidden atomic transitions using plasmonic nanostructures. Phys Rev A 2012;85:022501.
- [138] Lobanov SV, Weiss T, Dregely D, Giessen H, Gippius NA, Tikhadeev SG. Emission properties of an oscillating point dipole from a gold Yagi-Uda nanoantenna array. Phys Rev B 2012;85:155137.
- [139] Maksymov IS, Staude I, Miroshnichenko AE, Kivshar YS. Optical Yagi-Uda antennas. Nanophoton 2012;1: 65-81.
- [140] Jain PK, Eustis S, El-Sayed MA. Plasmon coupling in nanorod assemblies: optical absorption, discrete dipole approximation simulation, and exciton-coupling model. J Phys Chem B 2006;110:18243-53.
- [141] Decher G. Fuzzy nanoassemblies: toward layered polymeric multicomposites. Science 1997;277:1232-7.
- [142] Chen X, Lenhert S, Hirtz M, Lu N, Fuchs H, Chi L. Langmuir-Blodgett patterning: a bottom-up way to build mesostructures over large areas. Acc Chem Res 2007;40:393-401.
- [143] Iler RK. The chemistry of silica: solubility, polymerization, colloid and surface properties and the biochemistry. New York, USA: John Wiley and Sons Inc.; 1979.
- [144] Schmitt J, Decher G, Dressick WJ, Brandow SL, Geer RE, Shashidhar R, Calvert JM. Metal nanoparticle/polymer superlattice films: fabrication and control of layer structure. Adv Mater 1997;9:61-5.
- [145] Lavalle P, Voegel JC, Vautier D, Senger B, Schaaf P, Ball V. Dynamic aspects of films prepared by a sequential deposition of species: perspectives for smart and responsive materials. Adv Mater 2011;23:1191-221.
- [146] Rechberger W, Hohenau A, Leitner A, Krenn JR, Lamprecht B, Aussenegg FR. Optical properties of two interacting gold nanoparticles. Opt Commun 2003;220:137-41.

- [147] Prodan E, Radloff C, Halas NJ, Nordlander P. A hybridization model for the plasmon response of complex nanostructures. Science 2003;302:419-22
- [148] Vogelgesang R, Dmitriev A. Real-space imaging of nanoplasmonic resonances. Analyst 2010;135:1175-81.
- [149] Roy D, Fendler J. Reflection and absorption techniques for optical characterization of chemically assembled nanomaterials. Adv Mater 2004;16:479-508.
- [150] Okamoto T. Near field spectral analysis of metallic beads. In: Kawata S. ed. Near field optics and surface plasmon polaritons. Topics Appl Phys 2001;81:97-123. Heidelberg, Germany: Springer Verlag Berlin, 2001.
- [151] Smith DR, Schultz S, Markos P, Soukoulis CM. Determination of effective permittivity and permeability of metamaterials from reflection and transmission coefficients. Phys Rev B 2002;65:195104.
- [152] Menzel C, Rockstuhl C, Paul T, Lederer F, Pertsch T. Retrieving effective parameters for metamaterials at oblique incidence. Phys Rev B 2008;77:195328.
- [153] Pshenay-Severin E, Setzpfandt F, Helgert C, Hübner U, Menzel C, Chipouline A, Rockstuhl C, Tünnermann A, Lederer F, Pertsch T. Experimental determination of the dispersion relation of light in metamaterials by white-light interferometry. J Opt Soc Am B 2010;27:660-6.
- [154] Jie Y, Yonghua L, Pei W, Hai M. Integral fluorescence enhancement by silver nanoparticles controlled via PMMA matrix. Opt Commun 2011;284:494-7.
- [155] Muskens OL, Bachelier G, Fatti ND, Vallee F, Brioude A, Jiang X, Pileni MP. Quantitative absorption spectroscopy of a single gold nanorod. J Phys Chem C 2008;112:8917-21.
- [156] Van der Zande BMI, Pages L, Hikmet RAM, van Blaaderen A. Optical properties of aligned rod-shaped gold particles in poly(vinyl alcohol) films. J Phys Chem B 1999;103:5761-7.
- [157] Oates TWH, Wormeester H, Arwin H. Characterization of plasmonic effects in thin films and metamaterials using spectroscopic ellipsometry. Prog Surf Sci 2011;86:328-76.
- [158] Dolling G, Enkrich C, Wegener M, Soukoulis CM, Linden S. Simultaneous negative phase and group velocity of light in a metamaterial. Science 2006;312:892-4.
- [159] Zijlstra P, Orrit M. Single metal nanoparticles: optical detection, spectroscopy and applications. Rep Prog Phys 2011;74:106401.
- [160] Wahlstrom EE. Optical crystallography. New York, USA: John Wiley and Sons; 1969.
- [161] Scharf T. Polarized light in liquid crystals and polymers. New York, USA: John Wiley and Sons; 2006.
- [162] Husnik M, Klein MW, Feth N, König M, Niegemann J, Busch K, Linden S, Wegener M. Absolute extinction cross-section of individual magnetic split-ring resonators. Nature Photon 2008;2:614-7.
- [163] Sersic I, Tuambilangana C, Koenderink AF. Fourier microscopy of single plasmonic scatterers. New J Phys 2011;13:083019.
- [164] Taminiau TH, Karaveli S, van Hulst NF, Zia R. Quantifying the magnetic nature of light emission. Nature Commun 2012;3:979.
- [165] Courjon D, Bainier C. Near field microscopy and near field optics. Rep Prog Phys 1994;57:989.
- [166] Fischer UC, Pohl DW. Observation of single-particle plasmons by near-field optical microscopy. Phys Rev Lett 1989;62: 458-61.

- [167] Zayats AV, Smolyaninov II. Near-field photonics: surface plasmon polaritons and localized surface plasmons. J Opt A: Pure Appl Opt 2003;5:S16-50.
- [168] Wiederrecht GP. Near-field optical imaging of noble metal nanoparticles. Eur Phys J Appl Phys 2004;28:3-18.
- [169] Imura K, Okamoto H. Development of novel near-field microspectroscopy and imaging of local excitations and wave functions of nanomaterials. Bull Chem Soc Jpn 2008;81: 659-675.
- [170] Esteban R, Vogelgesang R, Dorfmüller J, Dmitriev A, Rockstuhl C, Etrich C, Kern K. Direct near-field optical imaging of higher order plasmonic resonances. Nano Lett 2008;8:3155-9.
- [171] Esslinger M, Dorfmüller J, Khunsin W, Vogelgesang R, Kern K. Background-free imaging of plasmonic structures with cross-polarized apertureless scanning near-field optical microscopy. Rev Sci Instrum 2012;83:033704.
- [172] Nelayah J, Kociak M, Stephan O, Garcia de Abajo FJ, Tence M, Henrard L, Taverna D, Pastoriza-Santos I, Liz-Marzan LM, Colliex C. Mapping surface plasmons on a single metallic nanoparticle. Nature Phys 2007;3:348-53.
- [173] Garcia de Abajo FJ. Optical excitations in electron microscopy. Rev Mod Phys 2010;82:209-75.
- [174] Von Cube F, Irsen S, Niegemann J, Matyssek C, Hergert W, Busch K, Linden S. Spatio-spectral characterization of photonic meta-atoms with electron energy-loss spectroscopy. Opt Mater Express 2011;1:1009-18.
- [175] Wegener M, Linden S. Shaping optical space with metamaterials. Physics Today 2010;63:32-6.
- [176] Kadic M, Guenneau S, Enoch S, Huidobro PA, Martin-Moreno L, Garcia-Vidal FJ, Renger J, Quidant R. Transformation plasmonics. Nanophoton 2012;1:51-64.
- [177] Alù A, Engheta N. Plasmonic and metamaterial cloaking: physical mechanisms and potentials. J Opt A: Pure Appl Opt 2008;10:093002.
- [178] Rockstuhl C, Scharf T. A metamaterial based on coupled metallic nanoparticles and its band-gap property. J Micros 2008;229:281-6.
- [179] Mühlig S, Farhat M, Rockstuhl C, Lederer F. Cloaking dielectric spherical objects by a shell of metallic nanoparticles. Phys Rev B 2011;83:195116.
- [180] West PR, Ishii S, Naik GV, Emani NK, Shalaev VM, Boltasseva A. Searching for better plasmonic materials. Laser & Photon Rev 2010;4:795-808.
- [181] Monti A, Bilotti F, Toscano A. Optical cloaking of cylindrical objects by using covers made of core-shell nanoparticles. Opt Lett 2011;36:4479-91.
- [182] Farhat M, Mühlig S, Rockstuhl C, Lederer F. Scattering cancellation of the magnetic dipole field from macroscopic spheres. Opt Express 2012;20:13896-906.
- [183] Alù A, Engheta N. Cloaking a sensor. Phys Rev Lett 2009;102:233901.
- [184] Fan P, Chettiar UK, Cao L, Afshinmanesh F, Engheta N, Brongersma ML. An invisible metal-semiconductor photodetector. Nature Photon 2012;6:380-5.
- [185] Tricarico S, Bilotti F, Vegni L. Reduction of optical forces exerted on nanoparticles covered by scattering cancellation based plasmonic cloaks. Phys Rev B 2010;82:045109.
- [186] Bilotti F, Tricarico S, Pierini F, Vegni L. Cloaking apertureless near-field scanning optical microscopy tips. Opt Lett 2011;36:211-3.

- [187] Hentschel M, Wu L, Schäferling M, Bai P, Ping E, Giessen H. Optical properties of chiral three-dimensional plasmonic oligomers at the onset of charge-transfer plasmons. ACS Nano 2012;6:10355-65.
- [188] Radke A, Gissibl T, Klotzbücher T, Braun PV, Giessen H. Three-dimensional bichiral plasmonic crystals fabricated by direct laser writing and electroless silver plating. Adv Mater 2011;23:3018-21.
- [189] Hentschel M, Schäferling M, Metzger B, Giessen H. Plasmonic diastereomers: adding up chiral centers. Nano Lett 2013:13:600-6.
- [190] Shen X, Asenjo-Garcia A, Liu Q, Jiang Q, García de Abajo FJ, Liu N, Ding B. 3D plasmonic chiral tetramers assembled by DNA origami. Nano Lett., submitted for publication.
- [191] Decker M, Klein MW, Wegener M, Linden S. Circular dichroism of planar chiral magnetic metamaterials. Opt Lett 2007:32:856-8.
- [192] Schäferling M, Dregely D, Hentschel M, Giessen H. Tailoring enhanced optical chirality: design principles for chiral plasmonic nanostructures. Phys Rev X 2012;2:031010.
- [193] Hentschel M, Schäferling M, Weiss T, Liu N, Giessen H. Three-dimensional chiral plasmonic oligomers. Nano Lett 2012;12:2542-7.
- [194] Gansel JK, Thiel M, Rill MS, Decker M, Bade K, Saile V, von Freymann G, Linden S, Wegener M. Gold helix photonic metamaterial as broadband circular polarizer. Science 2009;325:1513-5.
- [195] Yannopapas V. Negative index of refraction in artificial chiral materials. J Phys Condens Matter 2006;18:6883-90.
- [196] Müller J, Sönnichsen C, von Poschinger H, von Plessen G, Klar TA, Feldmann J. Electrically controlled light scattering with single metal nanoparticles. Appl Phys Lett 2002;
- [197] Large N, Abb M, Aizpurua J, Muskens OL. Photoconductively loaded plasmonic nanoantenna as building block for ultracompact optical switches. Nano Lett 2010;10:1741-6.
- [198] Campione S, Albani M, Capolino F. Complex modes and near-zero permittivity in 3D arrays of plasmonic nanoshells: loss compensation using gain. Opt Mater Express 2011;1:1077-89.
- [199] De Luca A, Grzelczak MP, Pastoriza-Santos I, Liz-Marzán LM, La Deda M, Striccoli M, Strangi G. Dispersed and encapsulated gain medium in plasmonic nanoparticles: a multipronged approach to mitigate optical losses. ACS Nano 2011;5:5823-9.
- [200] Noginov MA, Zhu G, Bahoura M, Adegoke J, Small CE, Ritzo BA, Drachev VP, Shalaev VM. Enhancement of surface plasmons in an Ag aggregate by optical gain in a dielectric medium. Opt Lett 2006;31:3022-4.
- [201] Gordon JA, Ziolkowski RW. The design and simulated performance of a coated nano-particle laser. Opt Express 2007;15:2622-53.
- [202] Gordon JA, Ziolkowski RW. CNP optical metamaterials. Opt Express 2008;16:6692-716.
- [203] Zheludev NI, Prosvirnin SL, Papasimakis N, Fedotov VA. Lasing spaser. Nature Photon 2008;2:351-4.
- [204] Noginov MA, Zhu G, Belgrave AM, Bakker R, Shalaev VM, Narimanov EE, Stout S, Herz E, Suteewong T, Wiesner U. Demonstration of a spaser-based nanolaser. Nature 2009;460:1110-2.

- [205] Wuestner S, Pusch A, Tsakmakidis KL, Hamm JM, Hess O. Overcoming losses with gain in a negative refractive index metamaterial. Phys Rev Lett 2010;105:127401.
- [206] Fang A, Koschny T, Wegener M, Soukoulis CM. Self-consistent calculation of metamaterials with gain. Phys Rev B 2009;79:241104.
- [207] Huang Z, Koschny T, Soukoulis CM. Theory of pump-probe experiments of metallic metamaterials coupled to a gain medium. Phys Rev Lett 2012:108:187402.
- [208] Silveirinha MG, Alù A, Edwards B, Engheta N. Overview of theory and applications of epsilon-near-zero materials. Chicago, IL: URSI General Assembly; 2008.
- [209] Alù A, Silveirinha MG, Salandrino A, Engheta N. Epsilonnear-zero metamaterials and electromagnetic sources: tailoring the radiation. Phys Rev B 2007:75:155410.
- [210] Silveirinha MG, Engheta N. Tunneling of electromagnetic energy through subwavelength channels and bends using e-near-zero materials. Phys Rev Lett 2006;97:157403.
- [211] Pendry JB. Negative refraction makes a perfect lens. Phys Rev Lett 2000;85:3966-9.
- [212] Paul T, Rockstuhl C, Menzel C, Lederer F. Anomalous refraction, diffraction and imaging in metamaterials. Phys Rev B 2009;79:115430.
- [213] Paul T, Menzel C, Rockstuhl C, Lederer F. Advanced optical metamaterials. Adv Mater 2010;22:2354-7.
- [214] Maslovski S, Tretyakov S, Alitalo P. Near-field enhancement and imaging in double planar polariton-resonant structures. J Appl Phys 2004;96:1293-300.
- [215] Alitalo P, Simovski C, Viitanen A, Tretyakov S. Near-field enhancement and subwavelength imaging in the optical region using a pair of two-dimensional arrays of metal nanospheres. Phys Rev B 2006;74:235425.
- [216] Sönnichsen C, Reinhard BM, Liphardt J, Alivisatos AP. A molecular ruler based on plasmon coupling of single gold and silver nanoparticles. Nature Biotech 2005;23: 741-5.
- [217] Anker JN, Hall WP, Lyandres O, Shah NC, Zhao J, Van Duyne RP. Biosensing with plasmonic nanosensors. Nature Mater 2008; 7:442-53.
- [218] Hering K, Cialla D, Ackermann K, Dörfer T, Möller R, Schneidewind H, Mattheis R, Fritzsche W, Rösch P, Popp J. SERS: a versatile tool in chemical and biochemical diagnostics. Analytical and Bioanalytical Chemistry 2008;390:113-24.
- [219] Derkacs D, Lim SH, Matheu P, Mar W, Yu ET. Improved performance of amorphous silicon solar cells via scattering from surface plasmon polaritons in nearby metallic nanoparticles. Appl Phys Lett 2006;89:093103.
- [220] Zijlstra P, Chon JWM, Gu M. Five-dimensional optical recording mediated by surface plasmons in gold nanorods. Nature 2009;459:410-3.
- [221] Kwon MK, Kim JY, Kim BH, Park IK, Cho CY, Byeon CC, Park SJ. Surface-Plasmon-Enhanced Light-Emitting Diodes. Adv Mater 2008;20:1253-7.
- [222] Liu N, Guo H, Fu L, Kaiser S, Schweizer H, Giessen H. Three-dimensional photonic metamaterials at optical frequencies. Nature Mater 2008;7:31-7.
- [223] Kern J, Großmann S, Tarakina NV, Häckel T, Emmerling M, Kamp M, Huang J-S, Biagioni P, Prangsma JC, Hecht B. Atomic-scale confinement of resonant optical fields. Nano Lett 2012;12:5504-9.